SIMPLIFYING WATERSHED MODELING

A Dissertation

Presented to the Faculty of the Graduate School

of Cornell University

In Partial Fulfillment of the Requirements for the Degree of

Doctor of Philosophy

by

Daniel Richard Fuka

January 2013

SIMPLIFYING WATERSHED MODELING

Daniel Richard Fuka, Ph. D.

Cornell University 2013

Obtaining representative meteorological data for an area, properly characterizing the physical characteristics of a watershed, and accurately representing the processes internal to watersheds can be complex. Several studies are presented that simplify the steps to obtain representative weather data, characterize the topography a watershed, and use this physical characterization to build a process based snowmelt model that requires no calibration to replace a calibration dependent temperature index based model. The objective of these studies is to present a suite of computational tools and proof of concept studies that simplify watershed modeling. First we present a method to quickly and easily obtain a 32-year record of meteorological forcing data for any location in the from the freely available Climate Forecast System Reanalysis dataset. Results from this analysis indicate that the CFSR data can reliably act as a first approximation of historical weather data over a watershed. The data consisting of precipitation, temperature, and other relevant weather information. Results show that using this dataset, can be as, or more, accurate than using weather records from the closest weather stations when using the Soil and Water Assessment Tool (SWAT) watershed model. The next two chapters describe two original software releases intended to provide watershed modeler with a suite of computational tools to better describe physical and chemical characteristics of a given watershed. The first, TopoSWAT, is a toolbox intended to characterize the topological properties of hydrological systems, and the second, SWATmodel, is an open-project porting of the

legacy SWAT watershed model to be widely distributed and run as a linear-model-like function on multiple operating systems (OS) and processor platforms within the R language. These software packages have resulted in significant simplification of the integration of physical characteristics into the SWAT modeling system and have made the SWAT modeling framework available to more users in multiple environments including those scientists dependent on the Unix and Mac Osx based operating systems. The final chapter presents an integration example of the previous chapters, building a more process-based snow accumulation and snowmelt routine to replace the temperature index based routine in the aforementioned SWAT modeling system. The results of this integration show that spatial snow distributions predicted by a more process-based model better matched observations from LandSat imagery and a SNOTEL station, and requires limited extra effort when initialized using the previously described TopoSWAT toolbox.

BIOGRAPHICAL SKETCH

Daniel Richard Fuka was born in Austin, TX, the youngest of four, to Mary and Louis Fuka. He grew up in New Mexico, and in 1991, obtained is B.S. in Horticulture from New Mexico State University. Daniel continued on to get his M.S. Engineering degree from Washington State University in 1995. From 1995 till 2010 Daniel moved his research into the private sector, first hired on as a research scientist and engineer at Quetzal Computation Associates, later Quetzal Biomedical Associates, and then in 2000 partnered in the weather commodities research group that would become Weather Insight, LLC. During this time the research group partnered and Daniel took on positions in the Air Routing Group companies and later Rockwell Collins. Not to be overlooked is the amazing partnership Daniel entered into when he met Melissa in 1995, who would become his loving and extremely patient wife in 1997, and who would understand the selling of the corporate partnerships, abandoning a great job, and moving to Ithaca, NY in 2010 to complete the mid-life crisis that is recapitulated in the following Dissertation.

Dedicated to John K. Prentice.

Without you, this chapter of my life would never have been written.

We loved you so much.

ACKNOWLEDGMENTS

First, I would like to acknowledge my wife, who supported me mentally, emotionally, and financially though this degree with little hesitation. I'd also like to thank my Mother and Father, who never doubted that I would be finished in a few months and never reminded me that the answer had not changed for years. Thanks to my sister Mary for reminding me every two weeks that I was not yet finished. Thanks to my friends in the soil and water lab especially Amy, Zachary, Brian and Ekrem who kept me balanced, and the friends I made working and teaching in Ethiopia. I want to thank my patient coauthors Todd, Art, Charlotte, and especially Tammo, as without him taking on special needs cases like myself, the opportunity start this degree would never have been possible.

Not to be overlooked is the support of Nancy, Debbi, Tami, Peggy, Steve Pacenka, as well as Jean Hunter and Brian Richards who helped me stay inside the box while thinking outside the box, and of course all the folks in Riley Robb that made life especially wonderful.

TABLE OF CONTENTS

LIST OF FIGURES

LIST OF TABLES

CHAPTER 1

INTRODUCTION

The focus of the research presented in this dissertation addressed a suite of new computational ideas and tools for simplifying watershed modeling. It is presented as four separate papers, chapters 2 through 5. In this introduction, a short overview is presented first, followed by a more in depth review. Chapter 2 describes a method of quickly and easily obtaining weather data, i.e., the hydrological forcing data, such as precipitation, temperature and other weather information. Chapter 3 describes a software "toolbox" that builds a better characterization of a watershed's physical properties for use in watershed modeling. We specifically focus on characterizing the topographic surface and soil properties and demonstrate how these data can lead to new modifications of the legacy Soil and Water Assessment Tool (SWAT - Arnold et al., 1998) watershed management model. With the atmospheric forcing and surface properties better characterized, chapter 4 is presented as a news item describing an open-project porting of the SWAT model to be widely distributed and run as a linear-model-like function[1] on multiple operating systems (OS) and processor platforms. In addition to simplifying the use of SWAT across computational platforms, the resulting SWATmodel package allows SWAT modelers to utilize the analytical capabilities, statistical libraries, modeling tools, and programming flexibility inherent to R. In

[1] The entire SWAT model, including parameter/HRU initialization, watershed delineation, model calibration, etc. can be called by a single function.

chapter 5, the surface characterization from chapter 3 is utilized as an essential component to a process-based snow accumulation and snowmelt routine, which can replace the temperature index (TI) based routine in the aforementioned SWAT modeling system.

Atmospheric forcing of watershed models

A common challenge in modeling watershed hydrology is obtaining accurate weather input data (e.g., Kouwen, et al., 2005; Mehta et al., 2004), often one of the most important drivers for watershed models (Obled et al., 1994; Bleeker et al., 1995). Weather is often monitored at locations outside the watershed to be modeled, sometimes at a long distance from the watershed. As a result, the available records may not meaningfully represent the weather actually occurring within the watershed. Moreover, weather records are seldom complete, which requires substituting other measurements or incorporating some sort of "estimated" precipitation. Thus, there is a need and, indeed, an opportunity to consider new, potentially simpler methods to obtain meteorological forcing data for watershed-scale modeling.

In chapter 2 we determine if multiyear global gridded representations of weather known as reanalysis data sets could be used as a complete, simple-to-extract, first approximation to the weather forcing information needed for modeling watersheds. We set three basic rules that needed to be met for dataset selection: i) an openly available global reanalysis dataset that included temperature and precipitation rate, ii) a spatial resolution on the order of 30km with sub-day temporal resolution, and iii) the

period of record should include several decades and extend to the present. For this study, we assess whether or not precipitation and temperature data derived from the National Centers for Environmental Prediction (NCEP) Climate Forecast System Reanalysis (CFSR - Saha et al., 2010) can be reliably used in watershed modeling relative to using the traditional weather station data approach. In addition we perform studies to answer the question: at what distance from the watershed does a weather station have to be such that CFSR provides more representative weather input than using station data?

Surface topography in watershed modeling

Topography plays a crucial role in many ecosystem and hydrological processes, which, in turn, influence ecosystem productivity and associated biogeochemical cycles (e.g., carbon-cycle, N-cycle). The movement of water within the landscape as surface (or near-surface) storm runoff and interflow is driven by gravity, topography and contributing area, which thereafter play roles in concentrating water flows that eventually generate the saturated (or near-saturated) areas where storm runoff is generated (Hewlett and Nutter, 1970; Dunne and Black, 1970). Other topographically-influenced factors that are hydrologically important include solar radiation (Swift, 1976; Tian et al., 2001; Fuka et al., 2012), local temperature, and precipitation (Bigler, 2007; Ahl et al., 2008), which play direct roles in snow accumulation, snowmelt, evaporation, transpiration and therefore plant productivity.

Several attempts have been made to modify the widely used SWAT model to incorporate a stronger representation of topography and therefore improve simulation of distributed runoff generation within a watershed (Easton et al., 2008, 2011), though resulting methods were probably too complex and time-intensive for many SWAT users to perform.

Presented in Chapter 3 is a method to simplify incorporating topographic attributes that are missing in the SWAT model. This toolbox allows users to incorporate topography into a standard SWAT model set-up without disrupting the watershed initialization procedures within the current ArcSWAT interface. We have built a single-step toolbox (ArcTools extension) that interfaces directly with ArcSWAT, processes the requisite data layers, updates the SWAT databases, and creates the SWAT parameter lookup tables. The resulting simplified toolbox, the 'TopoSWAT toolbox', allows SWAT modelers to incorporate topographic features important for watershed modeling, without any changes to the current ArcSWAT initialization system. This allows modelers to utilize some of the previously proposed versions of SWAT (e.g., Easton et al., 2008) or develop their own routines that require topographic parameters.

Bridging legacy models to new research tools

Environmental models have been invaluable for helping researchers understand complex environmental systems but they have largely existed as quasi-static entities that evolve much more slowly than the growth of scientific knowledge. Often times

this is because the model has been developed and coded into languages that, at the time, were considered modern. But, as years progress, those languages are replaced by more modern languages. The SWAT model (Arnold et al., 1998) has been used by many researchers to try to understand complex watershed processes and for developing management and policy decisions to protect the environment, natural resources, and human infrastructure. However, it is coded in a language that fewer researchers are learning and in a language that is becoming harder to integrate with modern languages and modern operating systems . As a result the SWAT model, actively supported by the US Department of Agriculture and Texas A&M, runs only on Microsoft® Windows, which hinders modelers requiring other operating systemss.

Chapter 4 presents a software porting (i.e. the conversion of software from one computational paradigm to others) of the SWAT model to be supported and maintained in the Comprehensive R Archive Network (CRAN) distributed "SWATmodel" package, which allows SWAT to be widely distributed and run as a linear-model-like function on multiple OS and processor platforms. This allows researchers anywhere in the world using virtually any OS to run SWAT. In addition to simplifying the use of SWAT across computational platforms, the SWATmodel package allows SWAT modelers to utilize the analytical capabilities, statistical libraries, modeling tools, and programming flexibility inherent to R with the benefit of not requiring expensive, proprietary software e.g., ArcGIS®, MATLAB®, Vensim®, etc. (Voinov and Brown Gaddis, 2008; Kourgialas et al., 2010).

Adding process based snow accumulation and melt to SWAT

In areas with high elevations and/or high latitudes, up to 80% of the annual streamflow originates from snowpack and snowmelt (Pagano and Garen, 2005; Yarnell et al., 2010). Climate change is expected to result in changes in the hydrology of many regions that have historically depended on snowfall as their primary water source. Thus, researchers rely on watershed models like SWAT for evaluating possible future changes in hydrology. Although it is often referred to as a ‘‘physically based’’ model (e.g., Srinivasan et al., 2010) and, indeed, many of the biogeochemical subroutines in SWAT are somewhat ‘‘process-based’’ (PB), it uses an empirical temperature index (TI) model to predict snowmelt. Unfortunately, TI-based methods require extensive calibration that cannot be applied outside the range of conditions for which it is calibrated (Fuka et al., 2012). Incorporating more physically based approaches into SWAT will improve our confidence that results are representative of actual environmental processes and not artifacts of calibration procedures.

Chapter 5 explores the benefits of integrating a simple, process-based, spatially distributed, snowmelt, and snow depth routine in SWAT2005, SWAT2009, and future versions of the model, requiring no additional input parameters and only one simple additional initialization step to the current initialization procedures (as outlined in chapter 3). We compare the agreement between modeled and measured stream discharge at the watershed outlet for the straight temperature index and the more process-based snowmelt versions of SWAT, and we show that, although both models

are able to perform similarly well at the basin outlet, only the PB model is capable of correctly representing the intra-basin spatial distribution of snow.

Concluding Remarks

The subject matter of this dissertation is an overall simplification of the steps required for modeling watersheds. This simplification is not a conceptual or computational simplification, but a simplification of the modeling process as, a PB snowmelt model is conceptually more complex, but operationally simpler than a TI snowmelt model, which is the topic of the last chapter. In the second chapter, a global historical weather dataset is introduced which has the potential of providing a simple single weather source as the first approximation of the weather conditions over a watershed anywhere in the world. In the third chapter, a toolbox is introduced to simplify building a better representation of a watershed's hydrological characteristics for use by the SWAT modeling system. In the forth chapter, the legacy modeling system SWAT is ported into an openly maintained and globally distributed R package allowing researchers with limited Fortran experience to more easily upgrade the empirical models of the past to their best process-based equivalents of the present.

REFERENCES

Ahl, R.S., Woods, S.W., Zuuring, H.R. 2008. Hydrologic Calibration and Validation of SWAT in a Snow-Dominated Rocky Mountain Watershed, Montana, USA. Journal of the American Water Resources Association, 44(6):1411-1430.

Arnold J.G., Srinivasan R., Muttiah R.S., Williams J.R. 1998. Large area hydrologic modeling and assessment Part I: Model development. Water Resources Bulletin. 34(1):73 89.

Bigler, C., Gavin, D.G. Gunning, C. Veblen, T.T. 2007. Drought Induces Lagged Tree Mortality in a Subalpine Forest in the Rocky Mountains. Oikos 116(12):1983-1994.

Bleeker, M., DeGloria, S.D., Hutson, J.L., Bryant, R.B., Wagenet, R.J. (January 01, 1995). Mapping atrazine leaching potential with integrated environmental databases and simulation models. Journal of Soil and Water Conservation, 50(4):388-394.

Dunne, T., Black, R. D. 1970. Partial area contributions to storm runoff in a small New England watershed. Water resources research, 6(5):1296-1311.

Easton, Z.M., Fuka, D.R., Walter, M.W., Cowan, D.M., Schneiderman, E.M., Steenhuis, T.S. 2008. Re-Conceptualizing the Soil and Water Assessment Tool (SWAT) Model to Predict Runoff From Variable Source Areas. Journal of Hydrology 348(3-4):279-291.

Easton, Z.M., Walter, M.T., Fuka, D.R., White, E.D., Steenhuis, T.S. 2011. A simple concept for calibrating runoff thresholds in quasi-distributed variable source area watershed models. Hydrological Processes, 25(20):3131-3143.

Fuka, D.R., Easton, Z.M., Brooks, E.S., Boll, J., Steenhuis, T.S., Walter, M.T. 2012. A Simple Process-Based Snowmelt Routine to Model Spatially Distributed Snow Depth and Snowmelt in the SWAT Model. Journal of the American Water Resources Association, 1-11. DOI: 10.1111/j.1752-1688.2012.00680.x

Hewlett, J.D., Nutter, W.L. 1970. The varying source area of streamflow from upland basins. p. 65–83. In Symposium on interdisciplinary aspects of watershed management. American Society of Civil Engineering, New York, N.Y

Kourgialas, N.N., Karatzas, G.P., Nikolaidis, N.P. 2010. An integrated framework for the hydrologic simulation of a complex geomorphological river basin. Journal of Hydrology, 381(3-4):308-321.

Kouwen, N., Danard, M., Bingeman, A., Luo, W., Seglenieks, F. R., Soulis, E. D. 2005. Case Study: Watershed Modeling with Distributed Weather Model Data. Journal of Hydrologic Engineering, 10(1):23-38.

Mehta, V.K., Walter, M.T., Brooks, E.S., Steenhuis, T.S., Walter, M.F., Johnson, M., Boll, J., Thongs, D. 2004. Evaluation and application of SMR for watershed modeling in the Catskill Mountains of New York State. Environmental Modeling and Assessment, 9(2):77-89.

Obled, C., Wendling, J., Beven, K. 1994. The sensitivity of hydrological models to spatial rainfall patterns: an evaluation using observed data. Journal of Hydrology, 159(1-4):305-333.

Pagano, T., Garen, D. 2005. A Recent Increase in Western US Streamflow Variability and Persistence. Journal of Hydrometeorology, 6(2):173-179.

Saha, S., Moorthi, S., Pan, H.L., Behringer, D., Stokes, D., Grumbine, R., Hou, Y.T., Chuang H.Y., Juang H.M.H., Sela J., Iredell M., Treadon R., Keyser D., Derber J., Ek M., Lord S., Van Den Dool, H., Kumar, A., Wang, W., Long, C., Chelliah, M., Xue, Y., Schemm, J.K., Ebisuzaki, W., Xie, P., Higgins, W., Chen, Y., Wu, X., Wang, J., Nadiga, S., Kistler, R., Woollen, J., Liu, H., Gayno, G., Wang, J., Kleist, D., Van Delst, P., Meng, J., Wei, H., Yang, R., Chen, M., Zou, C.Z., Han, Y., Cucurull, L., Goldberg, M., Liu, Q., Rutledge, G., Tripp, P., Reynolds, R.W., Huang, B., Lin, R., Zhou, S. 2010. The NCEP climate forecast system reanalysis. Bulletin of the American Meteorological Society, 91(8):1015-1057.

Srinivasan, R., Zhang, X., Arnold, J. 2010. SWAT Ungauged: Hydrological Budget and Crop Yield Predictions in the Upper Mississippi River Basin. Transactions of the ASABE, 53(5):1533-1546.

Swift, Jr., L.W., 1976. Algorithm for Solar Radiation on Mountain Slopes. Water Resources Research, 12(1):108-112.

Tian, Y.Q., Davies-Colley, R.J., Gonga, P., Thorrold Short, B.W. 2001. Estimating solar radiation on slopes of arbitrary aspect. Agricultural and Forest Meteorology 109(1):67–74.

Voinov, A.A., Brown Gaddis, E.J. (2008) Lessons for successful participatory watershed modeling : a perspective from modeling practioners. In: Ecological modeling, 216(2):197-207.

Yarnell, S.M., Viers, J.H. Mount, J.F. 2010. Ecology and Management of the Spring Snowmelt Recession. BioScience, 60(2):114-127.

CHAPTER 2

USING THE CLIMATE FORECAST SYSTEM REANALYSIS AS WEATHER INPUT DATA FOR WATERSHED MODELS[*]

Abstract

Obtaining representative meteorological data for watershed-scale hydrologic models can be difficult and time consuming. Land-based weather stations do not always adequately represent the weather, because they are often far from the watershed of interest, have gaps in their data series, or recent data is not available. This study presents a method for using the Climate Forecast System Reanalysis (CFSR) global meteorological data set to obtain historical weather data and demonstrates the application to modeling five watersheds representing different hydro-climate regimes. CFSR data are available globally for each hour since 1979 at a 38 km resolution. Results show that utilizing the CFSR precipitation and temperature data provide stream discharge simulations that are as good as or better than simulations using land based weather stations, especially when stations are more than 10 km from the watershed. The CFSR data could be particularly beneficial for watershed modeling in data-scarce regions and for modeling applications requiring real-time data.

---

[*] Fuka, D.R., MacAlister, C., Easton, Z.M., DeGaetano, A.T. Walter, M.T., Steenhuis, T.S. 2012. Using the Climate Forecast System Reanalysis to Improve Weather Input Data for Watershed Models. Hydrological Processes, <submitted, second revision>

Introduction

A common challenge in modeling watershed hydrology is obtaining accurate weather input data (Kouwen, et al., 2005; Mehta et al., 2004), often one of the most important drivers for watershed models (Obled et al., 1994; Bleecker et al., 1995). Weather is often monitored at locations outside the watershed to be modeled, sometimes at a long distance from the watershed. As a result, the available records may not meaningfully represent the weather actually occurring within the watershed. An additional complication is that rain gauge data are effectively point measurements, which may represent precipitation poorly across a watershed, particularly if there are large hydro-climatic gradients (WMO, 1985; Ciach, 2003). This is particularly true for small convective storms. Moreover, weather records are seldom complete, which requires substituting other measurements or incorporating some sort of "estimated" weather conditions. To remedy this, some researchers have utilized radar data to provide precipitation inputs in some hydrological modeling studies, especially for modeling flood events (Ogden and Julien, 1994; Habib et al., 2008), but these data pose their own challenges including discriminating different forms of precipitation such as hail, snow and rainfall and determining the appropriate relationship between radar reflectivity and rain rate (Villarin and Krajewski, 2010). Thus, there is a need to consider new methods to estimate weather conditions for watershed-scale modeling.

One possibility is to use multiyear global gridded representations of weather known as reanalysis data sets, of which there are several (Table 2.1). Ward et al. (2011) found

Table 2.1. Reanalysis datasets available to this project from the NCAR Computational and Information Systems Laboratory (CISL) Research Data Archive (RDA). All datasets include temperature. Note: Japanese 25 year, ECMWF 40 Year, and ECMWF Interim Reanalysis are restricted datasets not available to the public.

Reanalysis Dataset (CISL ID)	**Date Range**	**Time Step**	**PPT Field**	**Res**	**Coverage**
NCEP/NCAR (ds090.0)	1948-2010	6hr	PPT Rate	2.5^{o}	Global
NCEP/DOE R2 (ds091.0)	1979-2012	6hr	PPT Rate	1.875^{o} (~209km)	Global
NCEP N. American Regional (ds608.0)	1979-2012	3hr	PPT Rate	~32km	North America
NCEP 51-Year Hydrological (ds607.0)	1948-1998	3hr	Total PPT	0.125^{o}	Continental US
ECMWF 15 Year (ds115.5)	1979-1993	6hr	Strat. + Conv. PPT	1.125^{o}	Global
ECMWF 40 Year (ds117.0)	1957-2002	6hr	Strat. + Conv. PPT	1.125^{o}	Global
ECMWF Interim (ds627.0)	1979-2012	6hr	Strat. + Conv. PPT	0.703^{o}	Global
CFSR (ds093.1)	1979-present	1hr	PPT Rate	0.3125^{o} (~38km)	Global
Japanese 25-Year (ds625.0)	1979-2011	6hr	Total PPT	1.125^{o}	Global

NCEP/NCAR is the National Centers for Environmental Prediction
DOE is the Department of Energy.
PPT Rate is the precipitation rate.
Strat. + Conv. refers to stratiform plus convective forms of precipitation.
ECMWF is the European Centre for Medium-Range Weather Forecasts.

that the NCEP/NCAR (National Centers for Environmental Prediction and National Center for Atmospheric Research respectively) and the European Centre for Medium-Range Weather Forecasts' (ECMWF) 40 year (updated version of the ECMWF 15 year) datasets had significant variability between the reanalysis precipitation fields and suggested that higher spatial resolution data are likely better suited to capture higher frequency events when modeling small to moderate sized watersheds. We set four basic rules that needed to be met for dataset selection: i) an openly available global reanalysis dataset that included temperature and precipitation rate, ii) a spatial resolution on the order of 30km, iii) sub-day temporal resolution, and iv) the period of record should include several decades and extend to the present. For this study we chose the NCEP Climate Forecast System Reanalysis (CFSR) primarily because of its relatively high spatial resolution, global coverage and up-to-date temporal coverage.

The CFSR dataset consists of hourly weather forecasts generated by the National Weather Service's (NWS) NCEP Global Forecast System (GFS). Forecast models are reinitialized every six hours, (analysis-hours = 0000, 0600, 1200, and 1800 UTC) using information from the global weather station network and satellite derived products. At each analysis-hour the CFSR includes both the forecast data predicted from the previous analysis-hour, as well as the data from the analysis utilized to reinitialize the forecast models. The horizontal resolution of the CFSR is 38 km (Table 2.1, Saha et al., 2010). This dataset contains historic expected precipitation and temperatures each hour for any land location in the world. Moreover, since the

precipitation is updated in near-real-time every 6 hours, these data can provide real-time estimates of precipitation and temperature for hydrologic forecasting.

The objective of this study is to determine whether CFSR derived weather data can be reliably used as input data instead of traditional weather station data in predicting discharge from a watershed.

Methods and Site Descriptions

We performed two types of studies to evaluate the reliability of CFSR data in predicting watershed discharge. Both studies utilized an adaptation of the Soil and Water Assessment Tool (SWAT) model (e.g., Arnold et al., 1998) that has been ported to the R modeling language and available through the CRAN repository (R Core Team, 2012). The SWATmodel package (Fuka et al., 2012) was chosen because it is widely implemented operationally as well as in research, and the integration into the R modeling language allowed for us to automate the optimization process using powerful tools such as the Differential Evolution Optimization (DEoptim) package (Ardia and Mullen, 2009) also freely available through the CRAN repositories. The hydrological subroutines in SWAT utilize a combination of empirical and process-based modeling approaches. Although SWAT is designed to predict a wide array of soil and water quality and flux characteristics, we only considered stream discharge in these studies. Additionally, because we are running this model in a variety of hydro-climatic environments, we are not concerned here with specific process representation, which likely vary among our watersheds, but rather we utilize SWAT as a response-

function, i.e., we are only trying to predict the stream response to the weather input. We conceptualized each watershed as consisting of three equal size sub-basins, idealized by three identical hydrologic response units (HRUs) in each sub-basin. Each HRU was characterized by the calibration parameters in Table 2.2; note the values for these parameters were uniform across the whole basin. Dividing the watersheds into sub-basins facilitated stream channel routing within SWAT.

In Study 1, two watersheds (Table 2.3 Study 1) were selected that had previously published SWAT model results using weather data from nearby stations as input data (e.g., Easton et al., 2008; White et al., 2011). SWAT model performance using these weather datasets was compared to SWAT model runs using CFSR derived weather data. This first study evaluated how watershed models using CFSR derived weather data might compare to a typical modeling study where modelers aggregate multiple weather stations to derive or fill gaps in the weather data that is used in the watershed model.

In Study 2, three watersheds (Table 2.3 Study 2) were selected that had several weather stations located at increasing distances from the watershed outlet (Table 2.4). Discharge was predicted using SWAT for both CFSR and weather station data. This second study evaluated how model performance in predicting discharge may diminish with increasingly distant weather stations and determines how CFSR based results would diminish if interpolated at distances further from the watershed.

Table 2.2. Calibrated parameters used for Differential Evolution Optimization, with the optimization method and parameter range, or percent deviation for optimization.

Variable	Definition	Method[a]	Range/Percent
SFTMP	Snowfall temperature [C]	replace	-5 – 5 Deg. C
SMTMP	Snow melt base temperature [C]	replace	-5 – 5 Deg. C
SMFMX	Melt factor for snow on June 21 [mm H_2O/C-day]	replace	-5 – 5 Deg. C
SMFMN	Melt factor for snow on December 21 [mm H_2O/C-	replace	-5 – 5 Deg. C
TIMP	Snow pack temperature lag factor	replace	-5 – 5 Deg. C
GW_DELAY	Groundwater delay [days]	replace	1 - 180 Days
ALPHA_BF	Baseflow alpha factor [days]	replace	1 - 180 Days
SURLAG	Surface runoff lag time [days]	replace	1 - 180 Days
GWQMN	Threshold depth of water in the shallow aquifer [m]	replace	1 - 200 mm
LAT_TTIME	Lateral flow travel time [days]	replace	1 - 180 Days
ESCO	Soil evaporation compensation factor	replace	.2 - .99
EPCO	Plant uptake compensation factor	replace	.2 - .99
CN2	Initial SCS CN II value	replace	65 - 85
Depth	Soil layer depths [mm]	percent	50 – 150 %
BD	Bulk Density Moist [g/cc]	percent	50 – 150 %
AWC	Average available water [mm/mm]	percent	50 – 150 %
KSAT	Saturated conductivity [mm/hr]	percent	50 – 150 %
RCHRG_DP	Deep aquifer percolation fraction	replace	0 – 1.0
REVAPMN	Depth of water in the aquifer for revap [mm]	replace	0 – 500 mm
GW_REVAP	Groundwater "revap" coefficient	replace	0 - .2

[a] "replace" indicates values were replaced within an initial range published in the literature and "percent" indicates values were determined by adjusting the base initialization default variables by a certain percentage.

Table 2.3. Table of watershed basin identifiers, characteristics and locations.

	Name	USGS Gage	Area (km^2)	K-G[1] Class	Lat/Lon	Study Period	Gage Elev (m)	Location
Study 1	Town Br.	01421618	36.6	Dfb	42.36/-74.66	1998-2004	784	Hobart, NY, USA
	Gumera	NA	1200	Cwb	11.84/37.63	1995-2003	1800	Near Bahir Dar, Ethiopia
Study 2	Andreas Cr.	10259000	22.1	Csa	33.76/-116.55	2000-2010	380	Palm Springs, CA, USA
	Tesuque Cr.	08302500	30.0	BSk	35.74/-105.91	2000-2010	2170	Santa Fe, NM, USA
	Cross R.	01374890	43.8	Dfa	41.26/-73.60	2000-2010	158	Cross R., NY, USA

[1]The Köppen-Geiger climate classification (Peel et al., 2007): BSk = Semiarid, steppe, cold; Csa = Mediterranian, temperate, dry summer, hot summer; Dfb = Humid, cold, without dry season, warm summer; Dfa = Humid, cold, without dry season, cold summer; Cwb = Temperate, dry winter, warm summer; http://people.eng.unimelb.edu.au/mpeel/koppen.html

Table 2.4. Table of Global Historical Climatology Network (GHCN) weather stations used for Cross R. (a), Tesuque Cr. (b), and Andreas Cr. (c), including distance from USGS streamflow gage (Dist) as well as percentage of days with missing weather data (%Miss), and Time of Observation(TofOb) in local time. Negative distances indicate stations closer to the ocean for Andreas Cr. and Cross R.

a) Cross River, Cross River, NY, USA

Station Name	GHCN ID	Dist (km)	% Miss	TofOb
DANBURY MUNICIPAL AIRPORT CT US	USW00054734	15.4	3.2	24
WEST POINT NY US	USC00309292	33.4	0.9	7
BRIDGEPORT SIKORSKY MEMORIAL AIRPORT CT US	USW00094702	-41.2	0.0	24
NEW YORK LAGUARDIA AIRPORT NY US	USW00014732	-58.3	0.0	24
NEW YORK J F KENNEDY INTERNATIONAL AIRPORT NY US	USW00094789	-70.3	0.0	24
FALLS VILLAGE CT US	USC00062658	79.0	1.8	7
OAK RIDGE RESERVOIR NJ US	USC00286460	79.5	2.3	8
NEWARK INTERNATIONAL AIRPORT NJ US	USW00014734	-79.9	0.0	24
BAKERSVILLE CT US	USC00060227	81.6	0.1	7
BURLINGTON CT US	USC00060973	81.9	2.9	7
CANOE BROOK NJ US	USC00281335	-85.4	2.4	8
ROCK HILL 3 SW NY US	USC00307210	92.1	1.6	8

b) Tesuque Creek, Sante Fe, NM, USA

Station n Name	GHCN ID	Dist (km)	% Miss	TofObs
SANTA FE 2 NM US	USC00298085	14.8	8.4	20
GLORIETA NM US	USC00293586	21.4	4.9	16
SANTA FE CO MUNICIPAL AIRPORT NM US	USW00023049	21.5	2.0	24
PECOS NATIONAL MONUMENT NM US	USC00296676	28.8	1.0	16
ESPANOLA NM US	USC00293031	31.3	12.2	6
LOS ALAMOS NM US	USC00295084	39.8	3.3	24
GASCON NM US	USC00293488	44.6	5.4	17

c) Andreas Creek, Palm Springs, CA, USA

Station Name	GHCN ID	Dist (km)	% Miss	TofObs
PALM SPRINGS REGIONAL AIRPORT CA US	USW00093138	8.6	2.1	24
PALM SPRINGS CA US	USC00046635	9.3	2.3	16
HEMET CA US	USC00043896	-36.2	0.2	16
DESERT RESORTS REGIONAL AIRPORT CA US	USW00003104	38.2	0.4	24
BORREGO DESERT PARK CA US	USC00040983	59.9	0.6	8
HENSHAW DAM CA US	USC00043914	-61.7	1.2	7
TWENTYNINE PALMS CA US	USC00049099	62.5	1.4	15
REDLANDS CA US	USC00047306	-67.4	1.8	14
CARLSBAD MCCLELLAN PALOMAR AIRPORT CA US	USW00003177	-97.5	1.9	24

--Study 1

Two watersheds were chosen for this study: The Town Brook watershed (37 km^2) located in the Catskill Mountains New York State, US, and the Gumera Watershed (1200 km^2) in the headwaters of the Blue Nile River in Ethiopia (Table 2.3). Both watersheds have been modeled previously using SWAT (e.g., Easton et al., 2008, 2011; White et al., 2011). The weather station dataset for the Town Brook watershed was taken directly from the Easton et al. (2008) study, and the weather station dataset for the Gumera watershed was taken directly from the White et al. (2011) study. The Town Brook weather data set was developed over time by several researchers studying a wide variety of models (e.g., Mehta et al., 2004; Agnew et al., 2006; Lyon et al., 2006a, b; Schneiderman et al., 2007; Easton et al., 2008; Shaw and Walter, 2009; Easton et al., 2011). The original Town Brook weather data was primarily taken from the weather station at Stamford, NY, which was located just outside the northern watershed boundary, with gaps filled using weather data from the Delhi, NY and Walton, NY weather stations located 25 km and 45 km from the outlet of the watershed, respectively.

For the Gumera Watershed in Ethiopia, precipitation data from White et al. 2011 was utilized. This dataset was originally obtained from the National Meteorological Agency of Ethiopia using the three closest weather stations to the Gumera basin.

--Study 2

For the second study, we selected three small (10-20 km^2) watersheds that represented distinct US hydro-climatic regions (Karl and Koss, 1984, Table 2.3) and that had

several weather stations within a 100 km radius from the outlet with nearly complete daily records (Table 2.4).

All weather station data for this second study were downloaded using the National Climatic Data Center (NCDC) Interactive Map Application for daily datasets accessing the GHCN (Global Historical Climate Network, Menne et al., 2011) database of temperature, precipitation and pressure records managed by the NCDC, Arizona State University and the Carbon Dioxide Information Analysis Center (http://gis.ncdc.noaa.gov/map/cdo/ accessed 2012/09/01).

--CFSR data

CFSR data were obtained through the Data Support Section (DSS) of the Computational and Information Systems Laboratory (CISL) at the National Center for Atmospheric Research (NCAR) in Boulder, Colorado. For each catchment we interpolated the CFSR temperature and precipitation rate fields to the center of the catchment (the fields identified as tmp2m and prate, respectively). Daily maximum and minimum temperatures were determined from the hourly forecast values and daily precipitation rates were determined by summing precipitation over 24 hour periods. Maximum and minimum temperatures as well as precipitation were calculated using geographic midnight to midnight for each basins location. For the analysis using weather stations at different distances from a watershed, we interpolated CFSR data to the coordinates of each weather station.

--Statistical analysis

All simulations were calibrated to maximize the Nash-Sutcliffe Efficiency (NSE, Nash and Sutcliffe 1970) between observed and simulated stream discharge on a daily time step using the DEoptim package in the R computing environment (Ihaka and Gentleman, 1996; RDC Team, 2009). Streamflow at the Gumera watershed outlet was calibrated for an 8 yr period, from 1996 to 2003, and streamflow in Town Brook was calibrated for a 5 yr period from 1998 to 2002 to enable us to compare and contrast the results with prior published studies for these watersheds (Easton et al., 2008; White et al., 2011). For the remaining basins, streamflow at the watershed outlet was calibrated for an 11 yr, period from 2000 to 2010. In the DEoptim library, the number of guesses for the optimal value of the parameter vector (NP) was set to eight and the number of iteration cycles over NP guesses (itermax), was set to 200. Each optimization converged near iteration 100, so this value did not seem to influence the optimization. Seventeen model parameters were calibrated in during optimization (Table 2.2). For the second analysis, we bootstrapped our data to determine the variability in our model performance. To do this we sub-sampled 1000 random days from our time series and determined our mean and standard deviations in NSE from these data.

Results

--Study 1

For the Town Brook and the Gumera watersheds, the simulated stream discharge using CFSR (NSE = 0.63 and 0.71, respectively) were similar to or slightly better than the results using weather station data (NSE = 0.52 and 0.68, respectively), as seen in Table 2.5 and Figures 2.1 and 2.2. Hydrographs for the two watersheds in Figure 2.3

Table 2.5. Table of NSE for the CFSR interpolated to the center of each watershed, the closest weather station, and the best meteorological weather station based datasets. Best meteorological weather is either a composite of stations in the case of Town Brook and Gumera, or single weather station in the case of Andreas Cr. Tesuque Cr. and Cross River.

Name	Location	CFSR Center	Closest Met[1] Weather	Closest Met Distance	Best Met[2] Weather	Best Met Distance
Town Br.	Hobart, NY, USA	.63	NA	NA	.52	NA
Gumera	Bahir Dar, Ethiopia	.71	NA	NA	.68	NA
Andreas Cr.	Palm Springs, CA, USA	.71	.36	9km	.67	9km
Tesuque Cr.	Santa Fe, NM, USA	.49	.08	15km	.34	45km
Cross R.	Cross R., NY, USA	.67	.63	15km	.63	15km

[1] Closest meteorological station to the center of the watershed.

[2] Best performing meteorological station weather, or combination of weather stations in the case of Town Brook and Gumera.

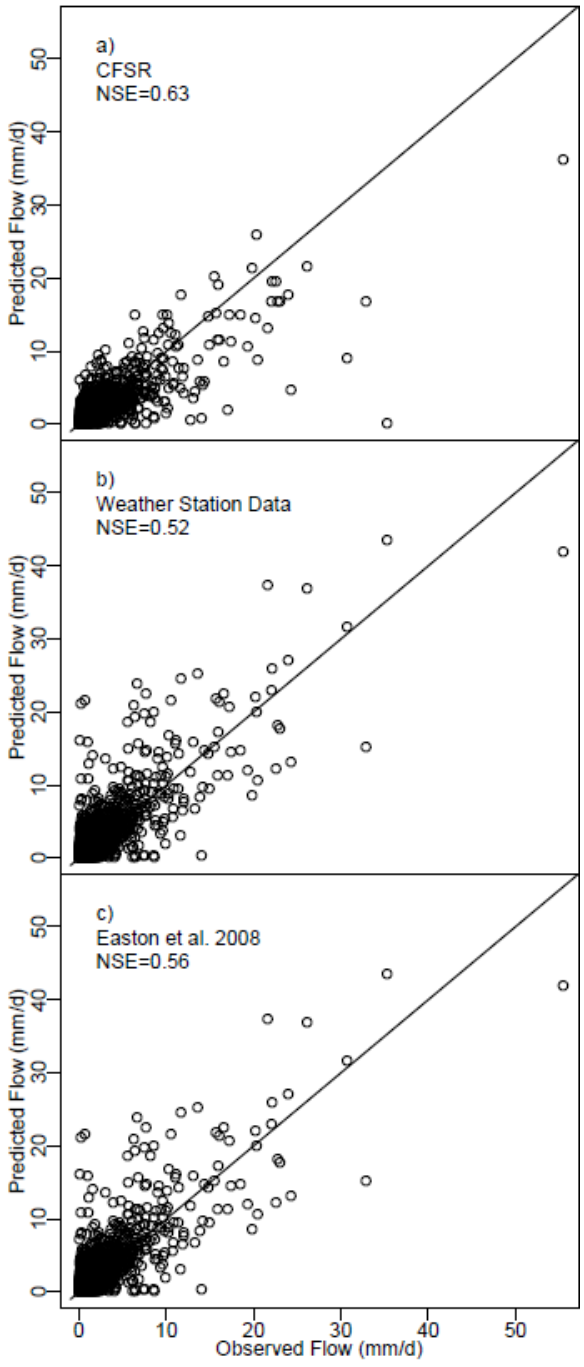

Figure 2.1a-c. Comparison of the simplified 9 HRU initializations in the Town Brook watershed for CFSR, a), ideal meteorological weather stations, b), and against the previous best values of the more complex SWAT model initialization shown in c). The simplified initialization performs similarly to the complex initialization, and there is a significant increase in performance when the CFSR meteorological data is used to force the SWAT model.

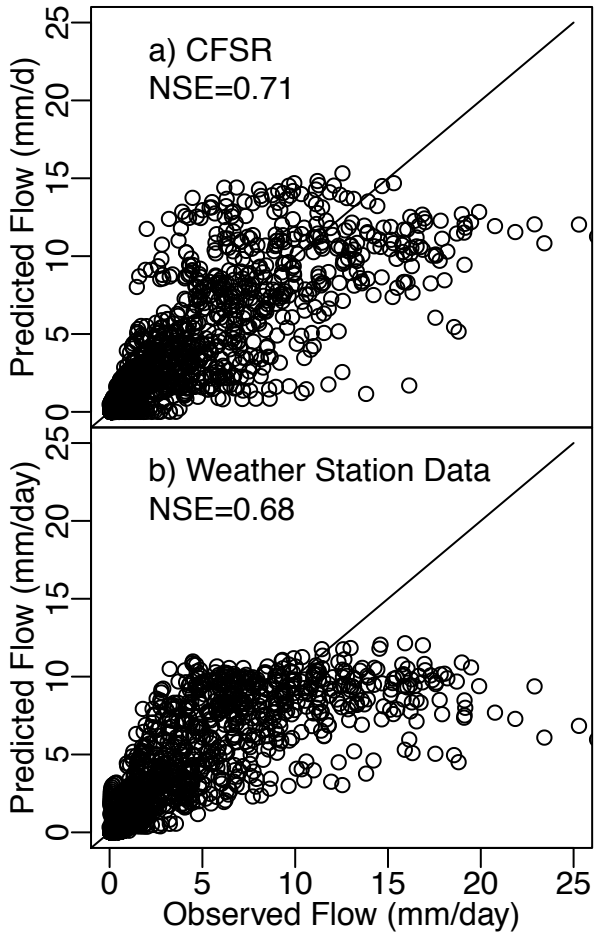

Figure 2.2a-b. Comparison of the simplified 9 HRU initializations in the Gumera watershed for CFSR a) and ideal meteorological weather stations b) and there is similar performance when the CFSR meteorological data is used to force the SWAT model vs. using the closest weather stations.

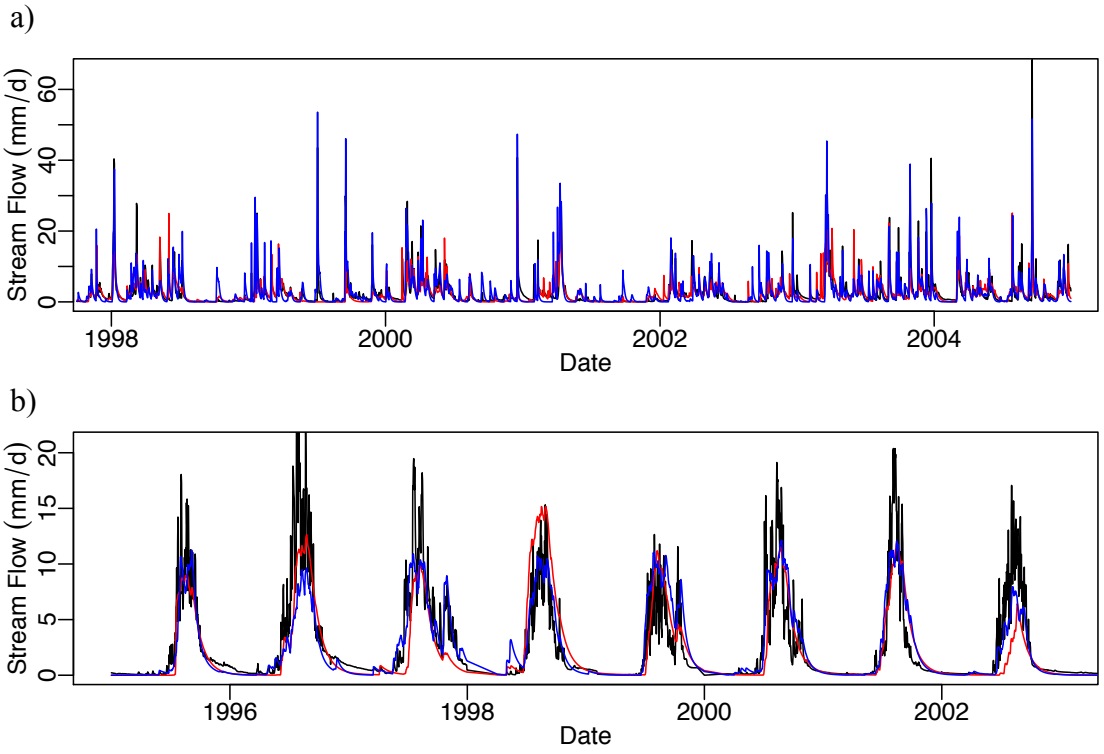

Figure 2.3a-b. Hydrographs for Town Brook (a) and Gumera (b) watersheds, showing the measured streamflow (black) with the CFSR-based prediction (red) and nearest weather station (blue).

also show similar behavior between the data sets for both watersheds. For Town Brook the optimized results for our SWAT initialization from this study are comparable to results from previous studies (Figure 2.1b,c) when using the same weather station data as the previous study. When using CFSR data the performance was slightly better as shown comparing Figure 2.1a to Figure 2.1b,c. For Gumera, the NSEs were similar to previous published studies (White et al. 2011).

--Study 2

For the Cross River, Tesuque Creek, and Andreas Creek in study 2, the modeled streamflow using CFSR data interpolated to the location of the stream gauge consistently had higher NSE values than the results generated using the nearest weather station (Table 2.5, and Figure 2.4, Figure 2.5, and Figure 2.6) with hydrographs of measured, closest weather station, and CFSR based weather data presented for each in Figure 2.7. Although we initially thought that model performance would diminish as the distance between the watershed and weather station increased, our results suggest somewhat more complex relationships. Figure 2.8 shows that in some cases (e.g, Tesuque Creek) weather stations located at a greater distance from the watershed actually provide better, or more representative estimates of weather, as indicated by model performance.

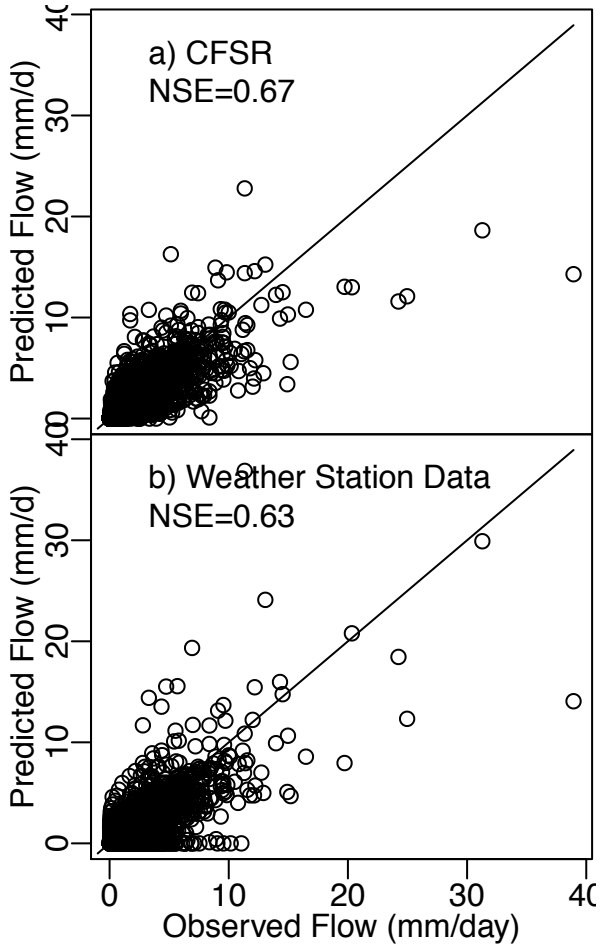

Figure 2.4a-b. Comparison of the simplified 9 HRU initializations in the Cross River watershed, a) shows the CFSR meteorological data results b) and ideal meteorological weather station results used to force the SWAT model.

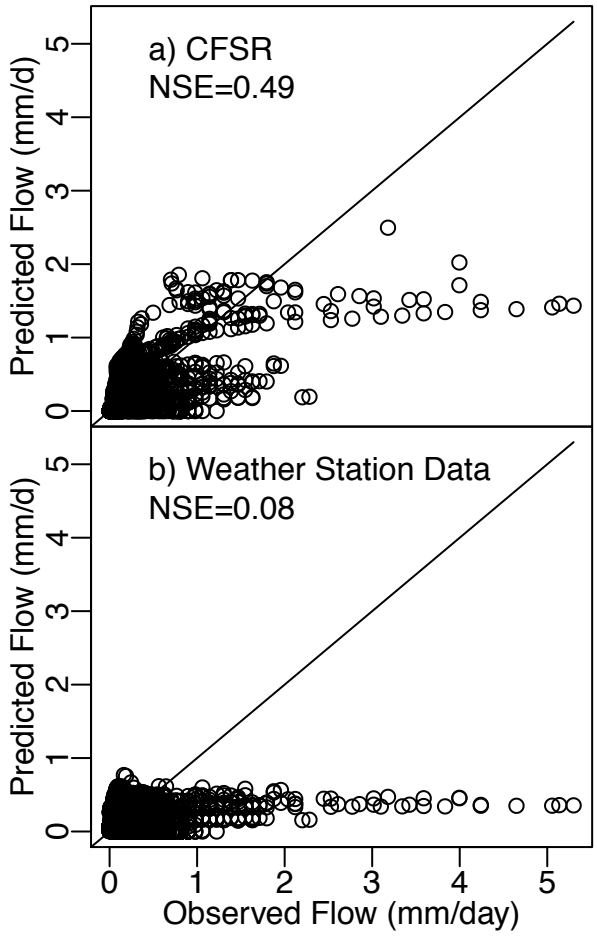

Figure 2.5a-b. Comparison of the simplified 9 HRU initializations in the Tesuque Creek Andreas Cr watershed, a) shows the CFSR meteorological data results and b) ideal meteorological weather station results used to force the SWAT model.

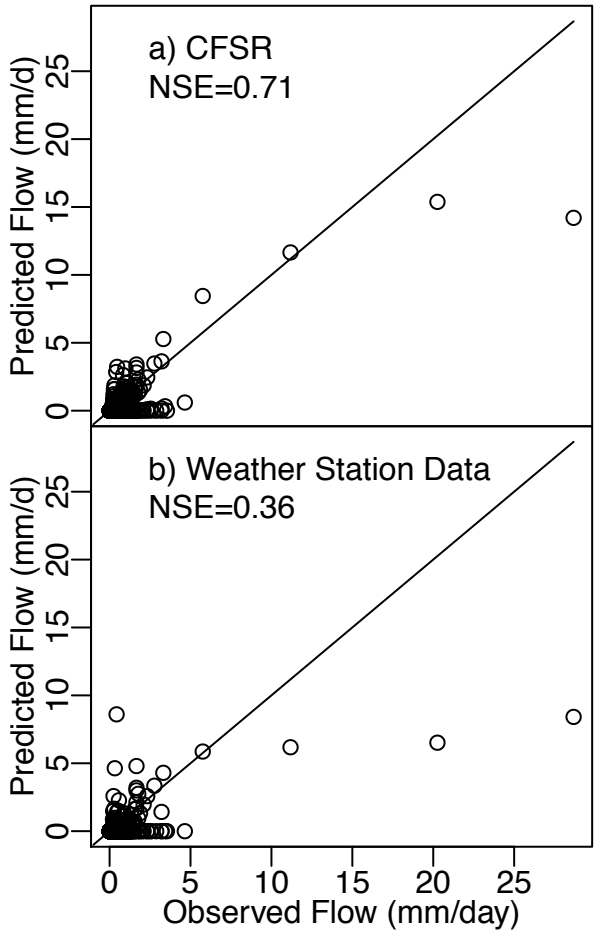

Figure 2.6a-b. Comparison of the simplified 9 HRU initializations in the Andreas Creek watershed, a) shows the CFSR meteorological data results and b) ideal meteorological weather station results used to force the SWAT model., Note, however in this case much of the good CFSR NSE performance is due to a few very large flow events.

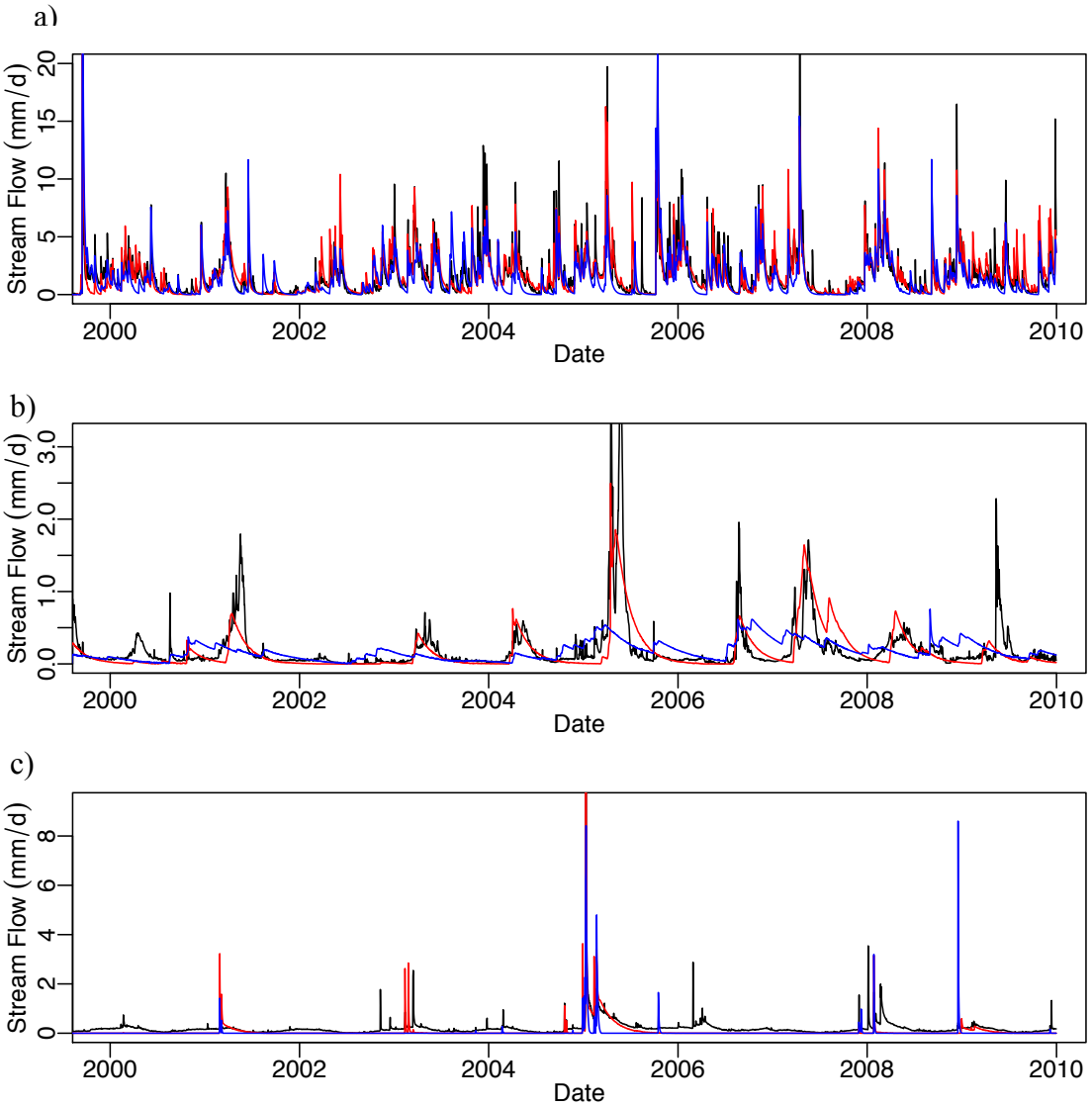

Figure 2.7. Hydrographs for Cross R. (a), Tesuque Cr. (b), and Andreas R. (c) showing the measured streamflow (black) with the CFSR-based prediction (red) and nearest weather station (blue).

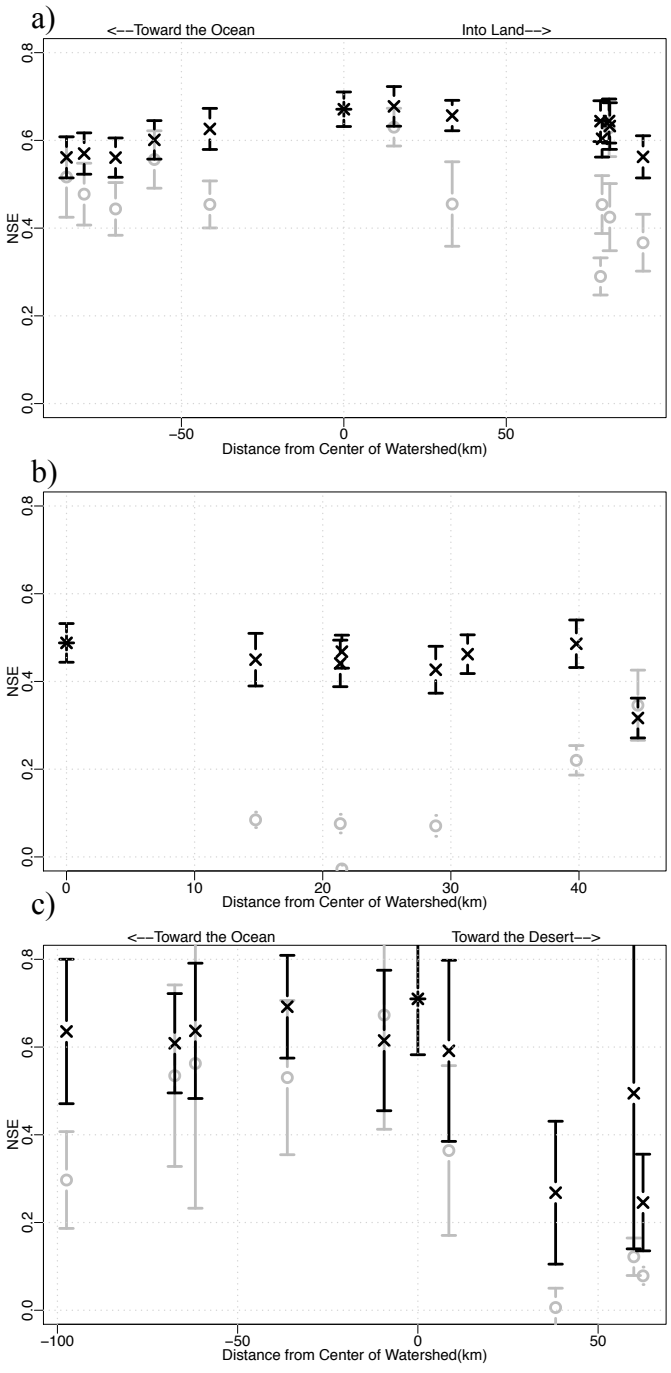

Figure 2.8a-c. Optimal NSE for the CFSR (x) and weather stations (circle) at various distances from the center of Cross R (a), Tesuque Cr. (b), and Andreas Cr. (c). Optimal NSE for CFSR interpolated to the center of the watershed is show with the asterisk (*) in each case. Negative distances indicate stations that are towards the Ocean (a and c only), with the exception of the "Palm Springs" station, which is placed in the negative side at -9.3km, to distinguish it from the "Palm Springs Regional Airport" station, at +8.6km. Error bars indicate +- 2 St. Dev. for 1000 bootstrap samples of predicted vs. observed results.

For Cross River and Andreas Creek, the NSE values declined less rapidly with increasing distance between the weather station and watershed moving towards the ocean than when considering stations further inland (Figure 2.8a,c). CFSR based results showed a similar pattern at Andreas Creek, but a more or less symmetrical decline in NSE at Cross River, presumably because there is a more rapid climatic transition inland from Andreas Creek relative to Cross River. For the Tesuque Creek watershed (Figure 2.8b) it appears that weather station elevation and land cover classification, rather than proximity to the watershed were the most important factors in determining representative weather patterns. For Tesuque Creek, the best weather stations were actually the two furthest from the watershed but were most similar (e.g., mountainous, forested area of similar elevation). Because the CFSR data represent averages over much larger areas than weather station data, CFSR appears able to maintain predictive capability even when interpolated to points far away from the watershed. Note, however, the relatively arid watersheds, Andreas Creek and Tesuque Creek, were difficult to model hydrologically (Figure 2.7b,c), possibly because large storm runoff events are triggered by small, localized events that are not well represented by the relatively coarse-scale CFSR data or weather station data. In the case of Andreas Creek, the NSE for the study might be somewhat misleading due to some extreme events (comparing Figure 2.6 with Figure 2.9). Figure 2.9, shows the performance of both CFSR and the closest weather station to decline substantially when considering smaller, more frequent storms.

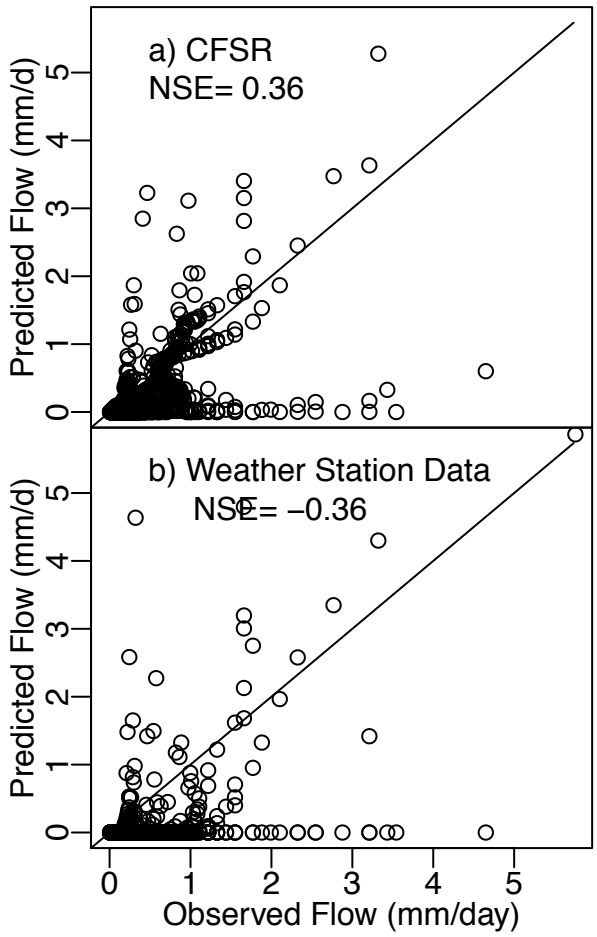

Figure 2.9a-b. Comparison of the simplified 9 HRU initializations in the Andreas Creek watershed for CFSR a) and ideal meteorological weather stations b) with extreme events shows that the CFSR meteorological data being used to force the SWAT model still performs better than using the closest weather station, though is a better representation of the lower performance when extreme events are removed as compared to Figure 2.6.

Discussion

In using CFSR as input to drive the SWAT model we obtained "satisfactory" (NSE > .5,) per Santhi et al. (2001) to "very good" (NSE > .65) per Saleh et al. (2000) results for predicted vs. observed flow on a daily time step, consistently better than using weather station records. Interestingly, the model results for Town Brook were better than those previously published by Easton et al. (2008), even though that study contained orders of magnitude more unique HRUs and were thus afforded more degrees of freedom in the SWAT calibration and used a weather record consisting of multiple stations.

The desert mountainous Southwestern climate in NM demonstrated the most significant benefits from using the interpolated CFSR dataset for several reasons. First, weather station density is substantially lower in this region relative to much of the rest of the conterminous US. This results in fewer basins having weather stations close enough to represent the streamflow well. More importantly, even with weather stations in close proximity to the watershed, the precipitation events, characteristically small cell based storm systems of short duration and low frequency were often not representative of weather occurring in the watershed. Stations within 10-20 km^2 had virtually no relationship with the observed streamflow for the basin (Figure 2.8b). As mentioned earlier, it is interesting that weather stations located at a greater distance produced better results than the closest stations, likely because they are located in similar terrain, i.e., more similar elevation and land cover classifications. In this case, the micro-climate similarities were significantly more important than the proximity of

the weather station. However, this type of climate is also challenging for the CFSR-based modeling because the high-intensity local events may be overly "dampened" in the relatively coarse-scale of the CFSR data (e.g., Figure 2.8b,c).

One reason the CFSR data may perform as well as it does for watershed modeling is because the weather data are effectively averaged over spatial scales that are more similar to many watershed extents; or, at least more similar than a typical point measurement of a weather station is to a watershed. Although most hydrology textbooks note that the magnitude of point rainfall needs to be adjusted when considering the rainfall over a larger surrounding area (e.g., Miller at al., 1973 cited in Dingman, 2002), few modelers do this explicitly, and often account for these differences during model calibration. Using the spatial CSFR data, such adjustments are not needed. As a result of the difference in spatial scales between CFSR data and weather station data direct comparisons between the two give little correlation. This is not surprising, and indeed has been noted in several other studies. For instance, Vasiloff et al. (2009) point out that wind, hail, missing gauge data, combined with storm paths make comparisons of weather station data against even much higher resolution radar and satellite precipitation products hard. In fact Mehta et al. (2004), demonstrated that weather gauges located closer together than the resolution of the CFSR have a low correlation with each other ($r^2 < 0.3$). However, when the CFSR data are developed there are automatic comparisons between CFSR and the ground-based weather data (Saha et al., 2010), which ensures some level of agreement.

One valuable attribute of the CFSR data is that it is globally available and will allow modelers access to weather data where there are no nearby weather stations. This is probably most valuable for data-poor regions such as in developing countries. In these regions, even when data are collected and archived, the effort and money required to access them can be substantial; the co-authors have personally experienced this specific difficulty in countries like India, Chile, and several countries in Africa. One reason for the inclusion of the Gumera watershed in Ethiopia was to make this point explicitly with a tangible example.

Another potentially valuable characteristic of the CFSR data for watershed modeling is that it is up-dated in real-time, including short-term forecasts (6 hours). This may facilitate more wide spread efforts in real-time or near-real-time hydrological modeling. This could be beneficial for predicting flood likelihood and location or for crop forecasting. It could also allow modelers to predict areas in a watershed with a high risk of generating runoff and where land managers might avoid environmentally risky activities (Walter et al., 2000; 2001; Agnew et al., 2006; Easton et al., 2008).

While we attempted to explore a wide range of hydro-climatic settings in this study, the next step will be to explicitly expand on these to determine where CFSR data work particularly well and where there may be problems. Also, although we looked at one large watershed (Gumera) and several on the order 40 km^2, the interplay between watershed size and CFSR data deserves more investigation. Probably the most valuable next-steps will be to apply CFSR to more physically-based modeling. The

objective of this study was limited to evaluating whether CFSR data could theoretically work for providing weather inputs to watershed modeling, especially where good weather station data are not available. Thus, we did not make any attempts to bias-correct the CFSR data. The way we employed the SWAT model, as a black-box response function, likely resulted in parameters calibrations that offset any systematic biases in the weather data.

Conclusion

This proof-of-concept study demonstrated that CFSR data could be reliably applied to watershed modeling across a variety of hydro-climate regimes and watersheds. Surprisingly, the CFSR data generally resulted in as good or better streamflow predictions as the best (often nearest) weather station. We speculate that this is, in part, because the CFSR data are averaged over areas comparable to watershed areas; at least more representative of watershed area than the area of a weather station. We note that this could be problematic for watersheds where the highest discharges are associated with very small, localized storms. In these cases, watershed modeling will be challenging regardless of the source of weather data. Adding CFSR data to the suite of watershed modeling tools provides new opportunities for meeting the challenges of modeling un-gaged watersheds and advancing real-time hydrological modeling.

Acknowledgements

Thanks to Eric White for sharing the simulation results and forcing data from White et al., 2011. We would like to also thank the funding support of the International Water

Management Institute (IWMI), an international research center under the Consultative Group on International Agricultural Research (CGIAR) umbrella, with funds from the Challenge Program for Water and Food. Development funding was provided from Raghavan Srinivasan at Texas AgriLife Research, a part of the Texas A&M System. Research funding was also provided from projects “Synthesis and Analysis of 13 CSREES CEAP projects”, project number USDA 2007-51130-03992, and “Regional Project for EPA REGION 1”, project number USDA-NIFA 2008-51130-19504.

REFERENCES

Agnew, L.J., Lyon, S., Gerard-Marchant, P., Collins, V.B., Lembo, A.J., Steenhuis, T.S., Walter, M.T. 2006. Identifying hydrologically sensitive areas: Bridging the gap between science and application. Journal Environmental Management, 78(1):63-76.

Ardia D., Mullen K., 2009. DEoptim: Differential evolution optimization in R. R package version 2.0-3. Available at: http://CRAN.R-project.org/package=DEoptim. Accessed September 3, 2010.

Arnold J.G., Srinivasan R., Muttiah R.S., Williams J.R. 1998. Large area hydrologic modeling and assessment Part I: Model development, Water Resources Bulletin. 34(1):73 89.

Ciach, G.J. 2003. Local random errors in tipping-bucket rain gauge measurements. Journal of Atmospheric and Oceanic Technology, 20(5):752–759.

Dingman, S.L. 2008. Physical Hydrology 2nd Ed. Waveland Press, In. Long Grove, IL 646 pages.

Easton, Z.M., Fuka, D.R., Walter, M.T., Cowan, D.M., Schneiderman, E.M., Steenhuis, T.S. 2008. Re-conceptualizing the Soil and Water Assessment Tool (SWAT) Model to predict runoff from variable source areas. Journal of Hydrology, 348(3-4):279-29.

Easton, Z.M., Walter, M.T., Steenhuis, T.S. 2008. Combined monitoring and modeling indicate the most effective agricultural best management practices. Journal of Environmental Quality, 37(5):1798–1809.

Easton, Z.M., Walter, M.T., Fuka, D.R. White, E.D., Steenhuis, T.S. 2011. A simple concept for calibrating runoff thresholds in quasi-distributed variable source area watershed models. Hydrological Processes, doi:10.1002/hyp.8032, 2011.

Fuka D.R., Walter, M.T, Easton, Z.M. 2012. EcoHydRology: A community modeling foundation for Eco-Hydrology. R package version 0.5.4. Available at: http://CRAN.R-project.org/package=SWATmodel. Accessed 08/01/2012

Gupta, H.V., Kling, H. 2011. On typical range, sensitivity, and normalization of Mean Squared Error and Nash-Sutcliffe Efficiency type metrics. Water Resources Research, 47(10) W10601.

Habib, E., Aduvala, A.V., Meselhe, E.A. 2008. Analysis of radar-rainfall error characteristics and implications for streamflow simulation uncertainty. Hydrological Sciences Journal, 53(3):568-587.

Karl, T., Koss, W.J. 1984. Regional and national monthly, seasonal, and annual temperature weighted by area, 1895-1983. Asheville, N.C: National Climatic Data Center.

Kouwen, N., Danard, M., Bingeman, A., Luo, W., Seglenieks, F. R., Soulis, E. D. 2005. Case Study: Watershed modeling with distributed weather model gata. Journal of Hydrologic Engineering, 10(1):23-38.

Lyon, S.W., M. McHale, M.T. Walter, T.S. Steenhuis. 2006a. Effect of runoff generation mechanism on estimating land use control of P concentrations. Journal of the American Water Resources Association, 42(3) 793-804.

Lyon, S.W., Lembo, A.J., Walter, M.T., Steenhuis, T.S. 2006b. Internet mapping tools make scientific applications easy. EOS, 87(38): 386.

Mehta, V.K., Walter, M.T., Brooks, E.S., Steenhuis, T.S., Walter, M.F., Johnson, M., Boll, J., Thongs, D. 2004. Evaluation and application of SMR for watershed modeling in the Catskill Mountains of New York State. Environmental Modeling and Assessment, 9(2):77-89.

Menne, M.J., I. Durre, R.S. Vose, B.E. Gleason, and T.G. Houston, 2011: An overview of the Global Historical Climatology Network daily database. Journal of Atmospheric and Oceanic Technology, submitted.

Miller, J.F., R.H. Fredrick, R.J. Tracey. 1973. Precipitation frequency atlas of the conterminous western United States (by states). Silver Spring, MD: US National Weather Service NOAA Atlas 2 (11 volumes).

Moriasi, D.N., Arnold, J.G., Van, L. M.W., Bingner, R.L., Harmel, R.D., Veith, T.L. 2007. Model evaluation guidelines for systematic quantification of accuracy in watershed simulations. Transactions of the ASABE, 50(3):885-900.

Nash, J.E., Sutcliffe, J.V. 1970. River flow forecasting through conceptual models. Part I a discussion of principles. Journal of Hydrology, 10(3):282-290.

Ogden, F.L., Julien, P.Y. 1994. Runoff model sensitivity to radar rainfall resolution. Journal of Hydrology, 158(1-2):1-18.

Peel M.C., Finlayson, B.L., McMahon, T.A. 2007. Updated world map of the Köppen-Geiger climate classification, Hydrology and Earth System Sciences, 11(5):1633-1644.

R Core Team. 2012. R: A language and environment for statistical computing. R Foundation for Statistical Computing, Vienna, Austria. ISBN 3-900051-07-0, URL http://www.R-project.org/.

Saha, S., Moorthi, S., Pan, H.L., Behringer, D., Stokes, D., Grumbine, R., Hou, Y.T., Chuang H.Y., Juang H.M.H., Sela J., Iredell M., Treadon R., Keyser D., Derber J., Ek M., Lord S., Van Den Dool, H., Kumar, A., Wang, W., Long, C., Chelliah, M., Xue, Y., Schemm, J.K., Ebisuzaki, W., Xie, P., Higgins, W., Chen, Y., Wu, X., Wang, J., Nadiga, S., Kistler, R., Woollen, J., Liu, H., Gayno, G., Wang, J., Kleist, D., Van Delst, P., Meng, J., Wei, H., Yang, R., Chen, M., Zou, C.Z., Han, Y., Cucurull, L., Goldberg, M., Liu, Q., Rutledge, G., Tripp, P., Reynolds, R.W., Huang, B., Lin, R.,Zhou, S. 2010. The NCEP climate forecast system reanalysis. Bulletin of the American Meteorological Society, 91(8):1015-1057.

Saleh, A., Arnold, J.G., Gassman, P.W., Hauck, L.M., Rosenthal, W.D., Williams, J.R., McFarland, A.M.S. 2000. Application of SWAT for the Upper North Bosque river watershed. Transactions- American Society of Agricultural Engineers, 43(5)1077-1088.

Santhi, C., Arnold, J.G., Williams, J.R., Dugas, W.A., Srinivasan, R., Hauck, L.M. 2001. TECHNICAL PAPERS - Validation of the SWAT Model on a large river Basin with point and nonpoint sources. Journal of the American Water Resources Association, 37(5):1169-1188.

Schneiderman, E.M., Steenhuis, T.S., Thongs, D.J., Easton, Z.M., Zion, M.S., Neal, A.L., Mendoza, G.F., Walter, M.T. 2007. Incorporating variable source area hydrology into a curve-number-based watershed model. Hydrological Processes, 21(25):3420-3430.

Shaw, S.B., Walter, M.T. 2009. Improving runoff risk estimates: Formulating runoff as a bivariate process using the SCS Curve number method. Water Resources Research, 45(3) W03404.

Thomas, R.K., Koss, W.J. 1984. Regional and national monthly, seasonal, and annual temperature weighted by area, 1895-1983. Historical Climatology Series 4-3, National Climatic Data Center, Asheville, NC, 38 pp.

Vasiloff, S.V., Howard, K.W., Zhang, J. 2009. Difficulties with correcting radar rainfall estimates based on rain gauge data: A case study of severe weather in Montana on 16–17 June 2007. Weather and Forecasting, 24(5):1334-1344.

Villarini, G., Krajewski, W.F. 2010. Review of the different sources of uncertainty in single polarization radar-based estimates of rainfall. Surveys in Geophysics, 3(1):107-129.

Ward, E., Buytaert, W., Peaver, L., Wheater, H. 2011. Evaluation of precipitation products over complex mountainous terrain: A water resources perspective. Advances in Water Resources, 34(10):1222-1231.

Walter, M.T., Walter, M.F., Brooks, E.S., Steenhuis, T.S., Boll, J., Weiler, K. 2000. Hydrologically sensitive areas: Variable source area hydrology implications for water quality risk assessment. Journal of Soil and Water Conservation, 55(3):277-284.

Walter, M.T., Brooks, E.S., Walter, M.F., Steenhuis, T.S., Scott, C.A., Boll, J. 2001. Evaluation of soluble phosphorus loading from manure-applied fields under various spreading strategies. Journal of Soil and Water Conservation, 56(4):329-335.

White, E.D., Easton, Z.M., Fuka, D.R., Collick, A.S., Adgo, E., McCartney, M., Awulachew, S.B., Selassie, Y.G., Steenhuis, T.S. 2011. Development and application

of a physically based landscape water balance in the SWAT Model. Hydrological Processes, 25(6):915-925, doi: 10.1002/hyp.7876.

CHAPTER 3

THE TopoSWAT TOOLBOX: INCLUSION OF TOPOGRAPHIC CONTROLS IN ARCSWAT INITIALIZATIONS*

Abstract

Topography exerts critical control on many hydrologic, geomorphologic, and environmental biophysical processes. In order to properly model such dynamics in the Soil and Water Assessment Tool (SWAT), we explicitly integrate topography into the initialization procedure with a purpose-built extension. This ArcMap® toolbox interfaces directly with ArcSWAT, to create multiple SWAT data layers, update the SWAT databases and generate the lookup tables required by the model. User defined data layers are processed in a single-step toolbox and include, aspect, elevation, and topographic index (TI), which are then intersected with the vector FAO Global Soils dataset. The toolbox then builds a soil raster layer at the resolution of the project's base Digital Elevation Model and creates the ArcSWAT required 'usersoil' database table along with the corresponding soil lookup table required to map the specific raster soil values to the soil parameters in the 'usersoil' database table. This toolbox effectively creates a new soil dataset that incorporates topographic features. This standardized method and toolset allows SWAT modelers to easily incorporate topographic features they believe are important for their catchments without requiring

---

* Fuka, D.R., MacAlister, C., Demissie, S.S, Walter, M.T., Easton, Z.M, Steenhuis, T.S. 2012. The TopoSwat Toolbox: Inclusion of Topographic Controls in ArcSWAT Initializations. Environmental Modeling and Software, <internal review>

any changes to the current ArcSWAT initialization system. Some of the topographic features may be necessary for process-based routines that one may want to incorporate into SWAT, e.g., energy-budget snowmelt modeling. However, such routines will need to be added to the SWAT model source code.

To demonstrate the toolbox we present two applications that require the SWAT model to reproduce distinctly different hydrological processes. The first case study includes slope aspect and elevation for predicting snowmelt and snow accumulation study in North Western Idaho, USA, and the second study models the variable source area hydrology of a mountainous region in Ethiopia requiring no changes in source code. In both case studies, the model results agreed better with field observations using the TopoSWAT toolbox initialization than using the standard SWAT initialization. This new SWAT toolbox adds flexibility to SWAT modeling with little extra effort on the part of modelers.

Introduction

Topography plays a crucial role in many ecosystem and hydrological processes which in turn influence ecosystem productivity and associated biogeochemical cycles e.g. carbon cycle. Wetland morphology is strongly determined by topography and associated hydrological connectivity (Mitsch and Gosselink, 2000), as are pedogenesis and catena or toposequence (Jenny, 1941, Foth, 1943, Lin, 2012). The movement of water within the landscape as surface (or near-surface) storm runoff and interflow is driven by gravity, topography and contributing area, which thereafter play roles in

concentrating water flows that eventually generate the saturated (or near-saturated) areas where storm runoff is generated (Hewlett and Nutter, 1970; Dunne and Black, 1970). Other topographically-influenced factors that are hydrologically important include solar radiation (Swift, 1976, Tian et al, 2001, Fuka et al. 2012), local temperature and precipitation (Bigler, et al., 2007; Ahl et al., 2008). These factors play direct roles in snow accumulation, snowmelt, evaporation, transpiration and therefore plant productivity.

While it is accepted that topography plays a critical role in numerous hydrologic and biogeochemical processes, many watershed models only use topographic features to delineate watershed, for example GWLF (Haith and Shoemaker, 2007) and SWAT (Arnold et al. 1998). Models that do incorporate topography, such as TOPMODEL (Beven et al., 1995), DHSVM (Wigmosta et al., 1994), and SMR (Zollweg et al., 1996; Frankenberger et al., 1999), have worked well in landscapes with saturation excess overland flow. Subsequently several attempts have been made to modify the widely used SWAT model to incorporate a stronger representation of topography and therefore improve simulation of distributed runoff generation within a watershed (Hewlett and Nutter 1970; Easton et al. 2008, 2011). Crop productivity models that require daily records of solar radiation, temperature, and precipitation (Hoogenboom et al., 1992; Hunt and Pararajasingham, 1995) can also be expected to benefit from the inclusion of topography to improve the surface energy budget for example.

The goal of this project was to develop a methodology incorporating the topographic attributes that we have stated are typically missing, into a standard SWAT model set-up without disrupting the watershed initialization procedures within the current ArcSWAT interface (Arc versions 9 and 10). To do this we built the missing features into the dataset of the 'soils' layer used within the watershed characterization of the SWAT model initialization. To make our application globally relevant we selected the Food and Agriculture Organization world soils dataset, as our soil data table and initial soil classification system. The data are based on the FAO-UNESCO Digital Soil Map of the World (DSMW) (FAO, 2007) and are freely available and used throughout the developing world where locally generated soil data are often lacking. To adequately represent topographic control on water redistribution within a watershed, we then included the generation of a Topographic Index (TI), elevation, slope, and aspect in the Soil Water Assessment Tool (SWAT) initialization by combining the attributes within the 'soil' layer.

We use the ArcSWAT GIS interface to initialize the SWAT model so that the generation and inclusion of TI requires the ability to manipulate and mesh the GIS files and databases that are the foundations of the ArcSWAT interface. Therefore, we have developed a single-step toolbox (ArcTools extension) that interfaces directly with ArcSWAT, processes the requisite data layers, updates the SWAT databases, and creates the SWAT lookup tables. This standardized method and toolset, the 'TopoSWAT toolbox', allows SWAT modelers to incorporate topographic features

they believe are important for their catchments, without requiring any changes to the current ArcSWAT initialization system.

The newly incorporated topographic features can be used to parameterize SWAT with the inclusion of Variable Source Area hydrology a methodology that adjusts the Curve Number (CN) based on TI within the parameterization of SWAT (SWAT-VSA Easton et al. 2008, SWAT-WB White et al., 2011); note: SWAT-WB requires alterations to the SWAT source code but SWAT-VSA does not. It also allows the user to initialize process based snowmelt routines, which also require changes to the SWAT source code (Fuka et al. 2012). Note, for clarification, the proposed initialization procedure that incorporates topographic parameters into SWAT does not require any changes to the SWAT source code.

Methodology

--Entry point into the ArcSWAT model initialization

The TopoSWAT toolbox uses two entry points into the standard ArcSWAT initialization: the DEM and the soil layer. The standard ArcSWAT model set-up, including watershed delineation and the definition of the parameterized units within the watershed on which calculations are based (Hydrological Response Units - HRUs), uses three initial data layers: (1) the Digital Elevation Model (DEM); (2) a soil layer; (3) a landuse layer. The TopoSWAT toolbox uses information contained intrinsically within the DEM, and the subsequent data layers generated from the DEM during watershed delineation, such as slope and contributing area, to generate the

Topographic Index, which is then added into the soil data layer, producing a 'new' soil layer that contains these 'bonus' properties. The properties are then incorporated in the 'HRU definition' and 'HRU analysis.' The toolbox necessarily requires a standard soil database format into which the topographic information is 'added.' We used the globally applicable FAO world soils dataset, as our soil data table and initial classification system. The United Nations University MWSWAT plugin for the Open Source GIS MapWindow (Waterbase, 2012) includes an ArcSWAT compatible version of the FAO global soils database. We utilized this information, available as a rasterized representation of the original DSMW vector format. In order to match the raster resolution of the base delineation digital elevation model (DEM) and prevent the development of numerically indistinct or incorrect transitional HRUs that result when grid projection, resolution and/or alignment is mismatched, we combined the vector layer with the MWSWAT developed SWAT parameter soils. The TopoSWAT toolbox incorporates topographic control on water redistribution within a watershed (as Topographic Index, defined as the quotient of contributing area and slope for any HRU) elevation, slope, and aspect are combined as attributes within the 'soil' layer. Incorporating wetness classes, slope aspect and elevation, involves the generation of a new 'soil' layer within SWAT initializations - the 'soil' layer which is used in HRU definition now contains more than soil properties. Adding these properties to existing classified soil layer within a watershed can multiply the number of 'soil classes' (and hence HRU's) exponentially and so similar topographic indices are finally classified into a user defined number of wetness classes (Table 3.1). The steps required to incorporate the properties into a standard set up are described below.

Table 3.1. Example of parsing of the HRU soil name 11210.1TI01A1Bd22-2bc with the relevant characters highlighted in bold italics.

Characters	**Connotation**
11210.1TI01A1Bd22-2bc	Run with VSA based model
1***1***210.1TI01A1Bd22-2bc	Run with PB snowmelt
11***21***0.1TI01A1Bd22-2bc	Elevation in 100s of meters
1121***0.1***TI01A1Bd22-2bc	Effective Depth Coefficient (WB method)
11210.1***TI01***A1Bd22-2bc	TI classification
11210.1TI01***A1***Bd22-2bc	East facing aspect
11210.1TI01A1***Bd22-2bc***	Original FAO soil name

Defining a global parameter in SWAT for use in the TopoSWAT toolbox

An important step in building the toolbox was to identify a SWAT model parameter in the Fortran code with no numerical significance within the program. The variable had to be globally accessible so that anyone intending to alter the base code set could determine each of the included attributes. In this case, we found that 'snam', the parameter identifying the soil name within the SWAT Fortran code base for each HRU, is used only for input and output and has no influence on any of the processes within the SWAT modeling system. For this study we introduce each topographic attribute, as well as a process-switch into the 'snam' parameter for each HRU using the first 4 characters as process switches. For example, in a VSA based model the first character of the soil name changes from 0 (indicating no changes from the original SWAT solution) to 1 (indicating a preference to run SWAT-VSA version) or 2 (running the SWAT-WB version). For process based snowmelt (Fuka et al. 2012) the second character of the 'snam' parameter changes from 0 to 1. Elevation, in hundreds of meters (about 10C in lapse rate), is included in characters 3 and 4 of the snam, so that 1800 m would have characters 3 and 4 set to '18'. The effective depth coefficient, a calibrated parameter in SWAT_WB (White et al 2011), uses characters 5 through 7, TI class uses characters 8 through 11, and D8 direction (1-8 representing east through south east in counter clockwise direction) identified in characters 12 and 13 (A1-8 for Aspect 1-8). Lastly the FAO soil name is added to the end of the string.

An example soil name of 11210.1TI01A1Bd22-2bc as described in table 3.1: 11 indicates that for the given HRU, you should run the VSA initialization for SWAT with process based snowmelt; the following 21 indicates elevation of 2100m, 0.1

indicates an effective depth coefficient of 0.1, which is used in calibration of SWAT-WB. The next 4 characters, TI01 indicate TI class of 1, and A1 indicates an east-facing slope.

--SWAT code modifications using HRU 'snam' parameter

As stated earlier, a modeler can make considerable use of the newly established topographic characteristics within the ArcSWAT interface, associating specific parameterizations to specific topographic characteristics identified during the HRU definition of "soils," and carried through to all of the underlying databases. For more advanced SWAT users adept in modifying the SWAT source code, the 'snam' parameter, and thus the topographic characteristics of each HRU, is available in all of the SWAT subroutines.

For an example of how this could be used within the SWAT Fortran code consider a simple modification to the temperature-index based snowmelt commonly used. Elevation increments can be used to alter the temperature with a simple adjustment to the temperature such as:

```
      integer :: snel, snc
C Reading in elevation in 100s of meters and D8 aspect.
      read(snam(j),'2X,I2,8X,I1') snel,snc
C Calculate new lapse rate based temperature
      owtmpav=tmpav(j)—(real(snel)-elevt(k)/100.0)*.55
```

where snel is the HRU elevation in 100s of meters; snam is the SWAT parameter for the soil name we use to implement our parameter space; owtmpav is the lapse rate adjusted temperature from elevt, the elevation of the temperature gage.

Similarly, to use the D8 aspect and HRU slope to determine the solar declination for energy budget based processes, one would add to the previous code segment the following:

```
C Calculate solar declination using D8 aspect,
C   day of year, and HRU slope
      slope_dec=-SIN((real(snc)-
1.0)*PI*2.0/8.0)*hru_slp(j)
      soldec=.4102*sin(2*3.1416/365*(iida-80))+slope_dec
```

where owtmpav in the fifth line of the code would be the adjusted temperature for the HRU's snowmelt routine based on a wet lapse rate of 5.50C/km. Solar declination (soldec, last line of code) is calculated using the slope of the HRU (slope_dec) and day of year (iida), parameters already within SWAT, with the newly introduced parameter snc, which is the HRU's D8 direction relative to due east clockwise.

--Steps in TopoSWAT toolbox development

While there are a number of options for language selection (ie VB, Python, .NET based languages), we developed the TopoSWAT toolbox in Python. Python is a widely used general-purpose, interpreted higher-level language requiring only modest programming experience to become competent. Initially the toolbox code was written to support the newer ESRI arcpy library. However this version can only support the latest ESRI ArcMAP distribution (version 10) and as it became apparent that many of our potential user group routinely use older versions (the 9.x family) we have prepared toolbox versions for ArcMAP 9x10. Because this is a project that is in alignment with the currently supported ArcSWAT projects, but is not currently within ArcSWAT, care and consideration is required to avoid 'breaking' existing systems while integrating changes.

With the current ArcSWAT initialization system, several of the required topographic elements are already calculated as part of the watershed delineation procedure and are available from the project's RasterStore geodatabase. To save processing time, the TopoSWAT toolbox uses those elements already calculated in the ArcSWAT initialization, and adds the new layers to the ArcSWAT project's RasterStore geodatabase. The steps required to build the topography layer are listed in order in Table 3.2. We list those steps we do not duplicate as performed under ArcSWAT, and those performed by the TopoSWAT toolbox under the "System" heading in Table 3.2. Depending on the dominant hydrological processes within the target watershed, it may be desirable to classify the wetness classes as an equal area distribution or as a

Table 3.2. Steps required to build a topography layer within the standard ArcSWAT watershed delineation procedure, and the additional steps performed by the TopoSWAT toolbox.

Step	Procedure	System
1	Calculating D8 aspect	ArcSWAT
2	Calculating slope	ArcSWAT
3	Calculating flow accumulation	ArcSWAT
4	Calculating TI	TopoSWAT
5	Splitting TI into equal area or weighted distribution classes	TopoSWAT
6	Splitting DEM into elevation gradient classes	TopoSWAT
7	Combining selected D8, TI, elevation	TopoSWAT
8	Build soil name and update project MDB	TopoSWAT
9	Building lookup table	TopoSWAT
10	Combine Soils/Slope/Landuses	ArcSWAT

distribution heavily weighted to the upper tail of the calculated TI. Therefore, the toolbox offers three classification options: first an equal area TI distribution, a 10 class wetness weighted distribution (WWD) of 1% 2% 4% 8% 14% 14% 14% 14% 14% 15%, and a WWD of 1 + 3 + 9 + 27+ 60, similar to the first, but decreased to cut the number of HRUs and resulting numerical requirements, while maintaining VSA. When the lookup table for the classified new layer is completed, this can be used normally as the soil layer in the standard SWAT initialization. Thus the only difference as compared to the original SWAT is the name of the soil i.e., the 'snam' parameter.

Application of the TopoSWAT toolbox

--Case Study 1: Snowmelt and Snow Accumulation

To demonstrate the usefulness of the TopoSWAT toolbox, we give an overview of two case studies that require the model to reproduce distinctly different hydrological processes requiring more topographic information than SWAT generally includes. The first study is from a region where snowmelt and snow accumulation are the dominant hydrological processes (Fuka at el. 2012) and uses the modification in the SWAT code introduced earlier. The second study is from an area of mountainous topography and monsoon climate where variable source area hydrology is the dominant hydrological process (Lui et al., 2008). In this example no changes to the SWAT code are required.

In the first case study the SWAT model is initialized using the TopoSWAT toolbox to delineate a 46km^2 watershed in Northwestern Idaho, United States. The TopoSWAT

toolbox is used to add D8 (DEM calculated eight directional flow direction) aspect and 200m elevation gradients to the FAO soils dataset. A standard ArcSWAT initialization is then performed, including the TopoSWAT toolbox D8 and elevation derived 'soil' layer and lookup table. The physically based (PB) snowmelt routine, implemented by Fuka et al. (2012), is then called to produce a more realistic spatiotemporal snowpack distribution as determined by comparing the PB model results to observations from LandSat imagery (Figure 3.1). For this example, the TopoSWAT toolbox interface made what had previously been a higher level GIS multi-day exercise into a single simple 1-minute process between the ArcSWAT 'Watershed Delineator' and 'HRU Analysis' procedures. Note, the standard SWAT with optimized temperature index snow melt parameters predicted no snow for the period shown in Figure 3.1 (standard SWAT prediction of 0mm snow depth not shown).

At this resolution, it is not possible to accurately determine snow depth using the satellite remotely sensed data, though Fuka et al. (2012) did show a relationship exists between the satellite channel brightness and the modeled snow depth using this methodology.

--Case Study 2: Run-off and Soil Moisture

In the second case study the SWAT model was established for the 1662km^2 Gilgel Abay sub-catchment of the Blue Nile watershed in the Ethiopian Highlands, which demonstrates the simulation of VSA type hydrology. The standard SWAT model was initialized first using the FAO global soil layer. Even though the FAO soil provides global soil information at 1:5,000,000 scale (FAO, 2007) for large-scale modeling, the

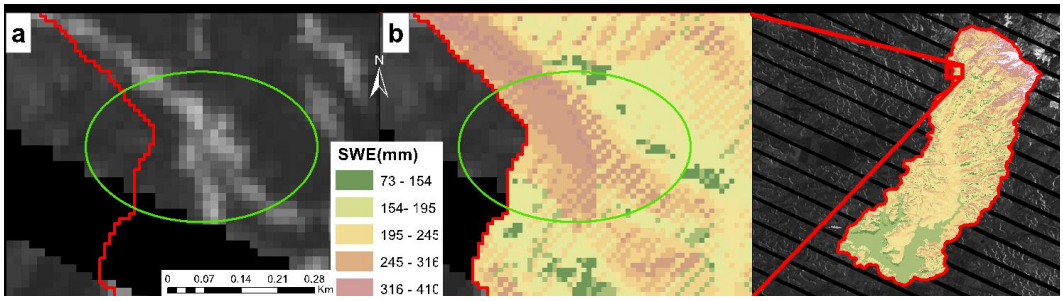

Figure 3.1. Spatial corroboration of snow distribution using LandSat 7 imagery from April 3, 2008, with ovals to highlight the same area in each scene. Left frame (a): LandSat 7 image shows hillslope snow distribution. Right frame (b): A physically based snowmelt model distinctly shows linear features of hillside snow that align with the LandSat 7 imagery.

Gilgel Abay watershed is only represented by one FAO soil class (Figure 3.2a). The topographic index classes were then added to the FAO soil dataset in a second, the TopoSWAT toolbox initialization of the same area while all other parameters remained identical. This multiplied the number of soil classes from one in the standard FAO soil layer initialization to ten in the TopoSWAT toolbox TI-soil layer initialization. Consequently, the number of hydrologic response units (HRUs) increased from 144 for standard ArcSWAT model to 1167 for topography-induced ArcSWAT model, significantly improving the internal representation of watershed attributes and processes. Figure 3.2a and 3.2b illustrate the soil layers of both initializations. Clearly the TI-soil layer provides a much more detailed representation of 'soil' distribution. Figures 3.2c and 3.2d indicate how this influences the representation of runoff in both subsequent ArcSWAT model outputs. The TopoSWAT toolbox provides a much more complex, detailed and, likely, realistic runoff distribution (Figure 3.2d). While the runoff amount is similar for identical land use and slope classes in standard ArcSWAT model with FAO soil (see Figure 3.2c), the spatial runoff distribution of the topography-induced ArcSWAT model follows the drainage and saturation pattern of the watershed (see Figure 3.2d), with more runoff generated around streams and lowland areas than upland parts of the watershed.

The annual changes in soil water content are illustrated in Figures 3.2e & and 3.2f for the standard and topography-induced ArcSWAT models respectively. This watershed is typical of mountainous watersheds located in monsoonal climates where the runoff dominantly occurs as overland flow from saturated valleys and impervious areas and

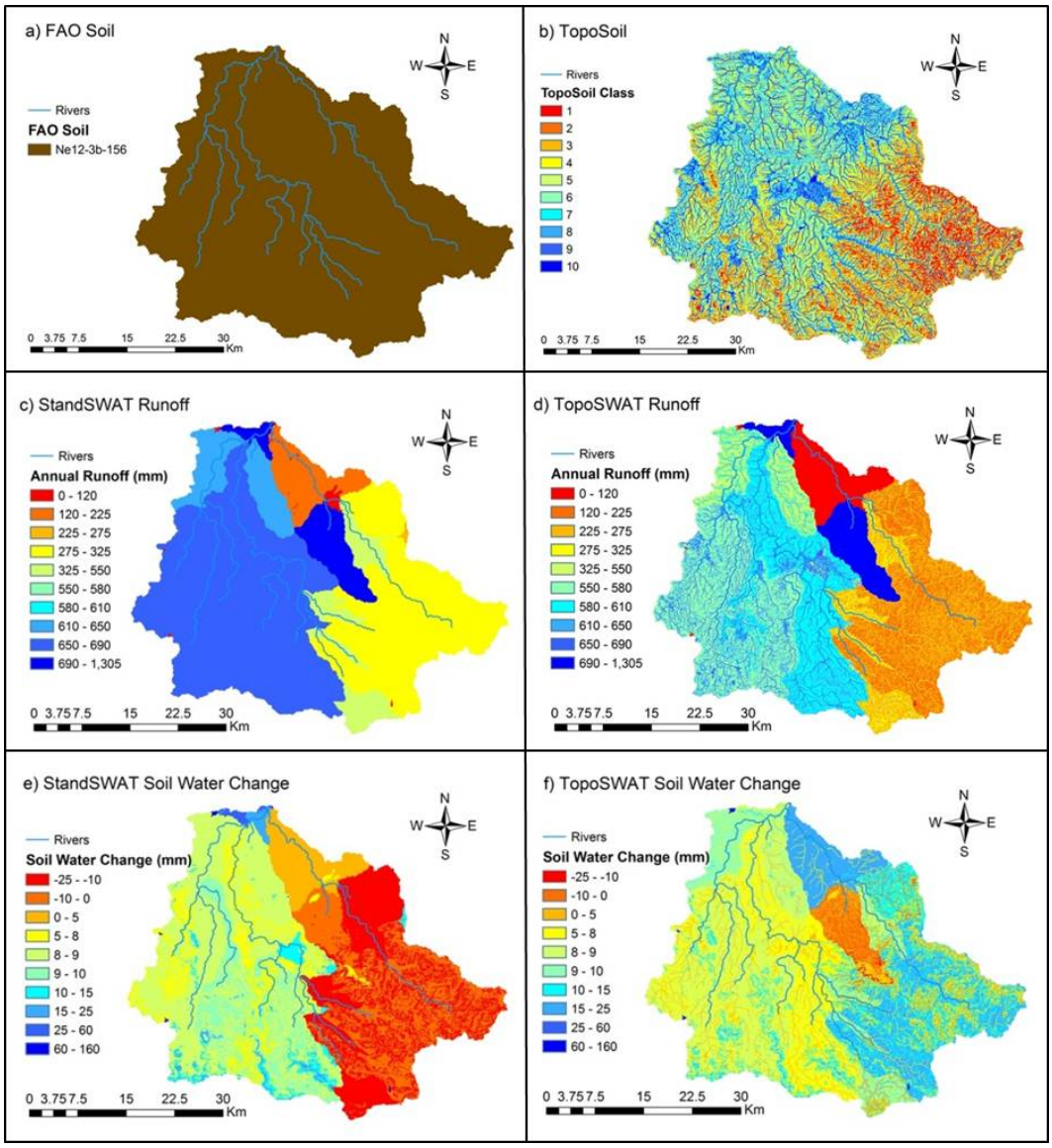

Figure 3.2a-f. SWAT model of Gilgel Abay, Blue Nile watershed, Ethiopia, initialized using a standard ArcSWAT setup with the FAO DSMW soil layer (a. SWAT), and with the TopoSWAT toolbox (b. TopoSoil); SWAT model outputs including runoff (c & d) and change soil moisture (e & f) for both model initializations.

the hillslope contribution is characterized by interflow (Steenhius et al., 2009). In this landscape rainfall rate rarely exceeds infiltration rate and runoff coefficient is negatively correlated with slope (Bayabil et al, 2010). With higher rate infiltration rates and lower water table on the hillslopes, the associate soil moisture is expected to have higher, positive seasonal change, as depicted in Figure 3.2f and contrary to Figure 3.2e. Surface and near-surface flows dominate the low slope lands and valley bottoms in the wet season, when the water table depth is consistently high. In these areas the watertable fluctuation and hence soil saturation is higher following pronounced alternation of dry and wet seasons of the monsoon climate. The main causes of runoff generation in such watersheds are direct precipitation runoff from saturated valleys and interflow from hillslopes. Therefore, the annual soil moisture changes in the valley bottoms and drainage networks are relatively lower and sometimes negative as that of Figure 3.2f.

Table 3.3 compares the performance of the two models. The standard SWAT and TopoSWAT toolbox based models both demonstrate comparable performance for simulated flow at the catchment outlet. While both models indicate that surface runoff is greater in lower parts of the watershed and plateau areas than on the hillslopes, the soil moisture dynamics produced with the standard SWAT and FAO soil layer (illustrated in Figure 3.2e), does not adequately represent the distribution of processes observed within the landscape. The TI-soil / TopoSWAT toolbox initialization represents a significant improvement in terms capturing internal watershed attributes and processes such as the spatial pattern of intra-annual soil moisture changes.

Table 3.3. Comparison of calibration performance of SWAT models for daily flow series (1998-2006) at Gilgel Abay catchment using FAO soil with a standard SWAT initialization (SWAT) and TI-soil layer using the TopoSWAT toolbox to initialize SWAT.

Performance Criteria	SWAT	TopoSWAT
[1]R^2	**0.69**	**0.79**
[2]NSE	**0.65**	**0.77**
[3]P-factor	**0.82**	**0.81**
[4]R-factor	**0.84**	**0.82**
[5]bR^2	**0.53**	**0.59**

[1]R^2 is the coefficient of determination of the measured and optimized daily flow data
[2]*NSE* is the Nash-Sutcliffe performance efficiency coefficient
[3]*P-factor* is the percentage of measured daily flow data bracketed by the 95% prediction uncertainty.
[4]*R-factor* is the average thickness of the 95% prediction uncertainty band divided by the standard deviation of measured daily flow data.
[5]bR^2 is the coefficient of determination multiplied by the slope of regression line between measured and optimized daily flow data. This coefficient is used as objective function for the Sequential Uncertainty Fitting (SUFI2) optimization algorithm of the SWAT-CUP (Abbaspour et al., 2004).

Discussion

The incorporation of topography into SWAT initializations, within the soil data layer in the ArcSWAT initialization routine, can improve the representation of controlling hydrological processes including snowmelt/accumulation and runoff generation. This addition of information into the basic data of watershed delineation increases complexity and, subsequently, the number of HRUs generated. However, in the case of energy dependent processes such as crop growth and snow accumulation and melt, we can better define the energy budget at the same resolution as the DEMs used to delineate the watershed. How well the spatial distribution of snow can be determined at field and hillslope resolutions is of great interest.

In the case of areas with limited soil data, incorporating topography into SWAT can improve the spatial representation of soil characteristics such as soil depth and organic carbon, as well as define the zonation of soils according to wetness, potentially related to the position within the landscape. As demonstrated in case study two, this can lead to more accurate modeling of the dominant hydrological processes.

The TopoSWAT toolbox allows modelers to simply and reliably incorporate topography into SWAT model initializations using a standard DEM for any land based location in the world.

In order to test its application in a wide range of landscapes, the toolbox is distributed freely to the ArcSWAT community, as well as others interested in derivative GIS

products. We are using the TI product in a number of other applications including landuse suitability analysis. This also helps to identify any 'bugs' and learn more about the usefulness of the tool. Therefore we invite any potential users to preview the video tutorial, and review the detailed procedures with working examples on how to use the toolbox, (available from the Easton Lab at Virginia Tech http://filebox.vt.edu/users/zeaston/Software.htm). In the future we hope topographic features will be incorporated within the ArcSWAT interface, maintained collaboratively by the USDA and Texas A&M University, thus rendering an external toolbox obsolete.

Conclusions

This article introduces an ArcMap toolbox that works directly alongside the ArcSWAT initialization platform to integrate the most important topographic characteristics required to best represent critical energy budget and hydrologic features of a watershed, as well as the potential redistribution of local soil characteristics, such as soil organic matter and soil horizon depths, which are often driven by topographic controls. The topography introduced into the initialization controls many watershed processes including hydrology, surface energy budgets and soil genesis. This ArcMap toolbox creates a new 'soil' layer, updates the SWAT databases with the base soil information for each of the new 'soil' classes, and generates the lookup tables required by the model. User defined data layers are processed in a single step toolbox and include, aspect, elevation, and topographic index (TI), which are then intersected with the vector FAO Global Soils dataset. This standardized method and toolset allows

SWAT modelers to incorporate topographic features they believe are important for their catchments, while not requiring any changes be made to the current ArcSWAT initialization system or the SWAT program source code.

The two case studies presented demonstrate: how incorporating elevation and aspect can better represent the spatial distribution of snow at the hillslope and field scale in the mountainous NW portion of the US Rocky Mountain Range; how local topography, incorporated using the TI, can benefit hydrological modeling of humid and semi humid monsoonal climates with saturation excess flow or organic soils, as found in the Blue Nile Basin in Ethiopia.

Lastly, the toolbox has been made available to the SWAT modeling community on a public repository; we are hopeful that the community finds enough benefit to incorporate these topographic elements into the ArcSWAT initialization interface maintained by USDA and Texas A&M University.

Acknowledgements

We would like to also thank the funding support of the International Water Management Institute (IWMI), an international research center under the Consultative Group on International Agricultural Research (CGIAR) umbrella, with funds from the Challenge Program for Water and Food.

REFERENCES

Abbaspour, K.C., Johnson, C.A. van Genuchten, M.Th., 2004. Estimating uncertain flow and transport parameters using a Sequential Uncertainty Fitting procedure. Vadose Zone Journal, 3(4):1340-1352.

Ahl, R.S., Woods, S.W., Zuuring, H.R. 2008. Hydrologic Calibration and Validation of SWAT in a Snow-Dominated Rocky Mountain Watershed, Montana, USA. Journal of the American Water Resources Association, 44(6):1411-1430.

Arnold J.G., Srinivasan R., Muttiah R.S., Williams J.R. 1998. Large area hydrologic modeling and assessment Part I: Model development. Water Resources Bulletin, 34(1):73 89.

Bayabil, H.K., Tilahun, S.A., Collick, S.A., Steenhuis, T.S. 2010. Are runoff processes ecologically or topographically driven in the Ethiopian Highlands? The case of the Mayabar watershed. Ecohydrology, 3(4): 457-466.

Beven, K.J., Lamb, R., Quinn, P., Romanowicz, R., Freer, J. 1995. TOPMODEL. In: Sing VP (Ed), Computer Models of Watershed Hydrology. Water Resources Publications, Colorado. pp. 627-668.

Bigler, C., Gavin, D.G. Gunning, C. Veblen, T.T. 2007. Drought Induces Lagged Tree Mortality in a Subalpine Forest in the Rocky Mountains. Oikos, 116(12):1983-1994.

Brutsaert, B., 2005. Hydrology: An Introduction. Cambridge: Cambridge University Press.

Dunne, T., Black, R. D. 1970. Partial area contributions to storm runoff in a small New England watershed. Water resources research, 6(5):1296-1311.

Easton, Z.M., Fuka, D.R., Walter, M.W., Cowan, D.M., Schneiderman, E.M., Steenhuis, T.S. 2008. Re-Conceptualizing the Soil and Water Assessment Tool (SWAT) Model to Predict Runoff From Variable Source Areas. Journal of Hydrology, 348(3-4):279-291.

Easton, Z.M., Walter, M.T., Fuka, D.R., White, E.D., Steenhuis, T.S. 2011. A simple concept for calibrating runoff thresholds in quasi-distributed variable source area watershed models. Hydrological Processes, 25(20):3131-3143.

FAO, 2007. http://www.fao.org/geonetwork/srv/en/metadata.show?id=14116 . Accessed 08/01/2012.

Foth, H.D., 1943. Fundamentals of Soil Science. 8th Edition (1990). John Wiley & Sons.

Frankenberger, J.R., Brooks, E.S., Walter, M.T., Walter, M.F., Steenhuis, T.S. 1999. A GIS-based variable source area hydrology model. Hydrological Processes, 13(6):805-822.

Fuka, D.R., Easton, Z.M., Brooks, E.S., Boll, J., Steenhuis, T.S., Walter, M.T. 2012. A Simple Process-Based Snowmelt Routine to Model Spatially Distributed Snow Depth and Snowmelt in the SWAT Model. Journal of the American Water Resources Association, 1-11. DOI: 10.1111/j.1752-1688.2012.00680.x

Haith, D.A., Shoenaker, L.L. 2007. GENERALIZED WATERSHED LOADING FUNCTIONS FOR STREAM FLOW NUTRIENTS. Journal of the American Water Resources Association, 23(3):471-478.

Hewlett, J.D., Nutter, W.L. 1970. The varying source area of streamflow from upland basins. p. 65–83. In Symposium on interdisciplinary aspects of watershed management. American Society of Civil Engineering, New York, N.Y

Hoogenboom, G., Jones, J.W., Boote, K.J. 1992. Modeling growth, development, and yield of grain legumes using SOYGRO, PNUTGRO, and BEANGRO: a review. Transactions of the ASAE, 35(6):2043-2056

Hunt, L.A., Pararajasingham, S. 1995. CROPSIM-WHEAT: a model describing the growth and development of wheat. Canadian Journal of Plant Science, 75(3):619-632.

Jenny, H. 1941. Factors of soil formation: a system of quantitative pedology. McGraw-Hill, NY.

Lin, H, 2012. Hydropedology: Addressing Fundamentals and Building Bridges to Understand Complex Pedologic and Hydrologic Interactions. Chapter 1. Henry Lin (Ed.) 2012. Hydropedology: Synergistic Integration of Soil Science and Hydrology. Academic Press/Elsevier. DOI: 10.1016/B978-0-12-386941-8.00001-0.

Liu, B.M., Collick, A.S., Zeleke, G., Adgo, E., Easton, Z.M., Steenhuis, T.S. 2008. Rainfall-discharge relationships for a monsoonal climate in the Ethiopian highlands. Hydrological Processes, 22(7):1059-1067.

Mitsch, W.J., Gosselink, J.G. 2000. Wetlands. 3rd edition, John Wiley and Sons, NY.

Moore, I.D., Gessler, P.E., Nielsen, G.A., Peterson, G.A. 1993 Soil Attribute Prediction Using Terrain Analysis, Soil Science Society of America Journal, 57(2):443-452.

Sørensen, R. Zinko, U. Seibert, J. 2005. On the calculation of the topographic wetness index: evaluation of different methods based on field observations. Hydrology and Earth System Sciences, 2(4):1807–1834.

Steenhuis, T.S., Winchell, M., Rossing, J., Zollweg, J.A., Walter, M.F. 1995. SCS Runoff Equation Revisited for Variable-Source Runoff Areas. Journal of Irrigation and Drainage Engineering, 121(3):234-238.

Steenhuis, T.S., Collick, A.S., Easton, Z.M., Leggesse, E.S., Bayabil, H.K., White, E.D., Awulachew, S.B., Adgo, E. and Ahmed, A.A., 2009. Predicting discharge and sediment for the Abay (Blue Nile) with a simple model. Hydrological Processes, 23, 3728-3737.

Swift, Jr., L.W., 1976. Algorithm for Solar Radiation on Mountain Slopes. Water Resources Research, 12(1):108-112.

Tian, Y.Q., Davies-Colley, R.J., Gonga, P., Thorrold Short, B.W. 2001. Estimating solar radiation on slopes of arbitrary aspect. Agricultural and Forest Meteorology, 109(1):67–74.

Walter, M.T., Brooks, E.S. McCool, D.K., King, L.G., Molnau, M., Boll, J. 2005. Process-Based Snowmelt Modeling: Does It Require More Input Data Than Temperature-Index Modeling? Journal of Hydrology, 300(1-4):65-75.

Waterbase, 2012. Available at: http://www.waterbase.org/home.html. Accessed 08/01/2012.

White, E.D., Easton, Z.M., Fuka, D.R., Collick, A.S., Adgo, E., McCartney, M., Awulachew, S.B., Selassie, Y.G., Steenhuis, T.S. 2011. Development and Application

of a Physically Based Landscape Water Balance in the SWAT Model. Hydrological Processes, 25(6):915-925, doi: 10.1002/hyp.7876.

Wigmosta, M.S., Vail, L.W., Lettenmaier, D.P. 1994. A distributed hydrology-vegetation model for complex terrain. Water resources research, 30(6):1665-1680.

Zollweg, J.A., Gburek, W.J., Steenhuis T.S. 1996. SMoRMod - A GIS-integrated rainfall-runoff model. Transactions of the ASAE, 39(4):1299-1307.

CHAPTER 4

SWATmodel: A MULTI-OS, MULTI-PLATFORM SWAT MODEL PACKAGE IN R*

Abstract

The Soil and Water Assessment Tool (SWAT) model (Arnold et al., 1998) is a popular watershed management tool. Unfortunately, the SWAT model actively supported by the US Department of Agriculture and Texas A&M runs only on Microsoft® Windows, which hinders modelers that use other operating systems (OS). This paper introduces the Comprehensive R Archive Network (CRAN) distributed "SWATmodel" package which allows SWAT to be widely distributed and run as a linear-model-like function on multiple OS and processor platforms. This allows researchers anywhere in the world using virtually any OS to run SWAT. In addition to simplifying the use of SWAT across computational platforms, the SWATmodel package allows SWAT modelers to utilize the analytical capabilities, statistical libraries, modeling tools, and programming flexibility inherent to R.

---

* Fuka, D.R., Easton, Z.M, Archibald, J.A.,MacAlister, C., Walter, M.T., Steenhuis, T.S. 2012. SWATmodel: A multi-OS, multi-platform SWAT model package in R. Environmental Modeling and Software, <submitted, second revision>

Software Availability

Name of software: SWATmodel
Concept: D.R. Fuka, Z.M. Easton, J.A. Archibald, M.T. Walter,
Programing: D.R. Fuka, Z.M. Easton, J.A. Archibald, M.T. Walter
Availability: install.packages("SWATmodel"), All CRAN, http://cran.r-project.org/
Year first available: 2011
Software required: R

News Item

The Soil and Water Assessment Tool (SWAT) (e.g., Arnold et al., 1998), which is in the public domain, is commonly used to help predict the effect of Best Management Practices (BPMs) on water, sediment, nutrient and pesticide yields. The model is used by many planning and regulatory agencies both in the US and abroad. Unfortunately, SWAT is only actively supported for Microsoft® Windows. Also, the model is developed using FORTRAN, which has steadily lost popularity to higher level languages. This is contributing to the gap between "new" research and modeling, as new research increasingly relies on higher level programming languages than "legacy" models which are often developed in FORTAN or C. The open source, relatively high level, R-language may provide a bridge that allows modelers around the world to easily access and run "legacy" models, like SWAT, and share "new" libraries, packages, data, code, and model output.

R is an open source, freely available computational system, initially developed as a statistical analysis tool to serve an alternative to the commercially available statistical analysis software, S. R has evolved into a sophisticated programming language supporting object-oriented programming. As a computational tool, R performs comparably to MATLAB; in statistical functioning it resembles popular software like

S and SAS. Also, R offers excellent language interoperability and can, through various extensions, access codes written in C, C++, FORTRAN 77, Fortran 9x, Objective C, Objective C++, Java, MATLAB, and others. The platform flexibility fosters multifarious model applications (e.g., TOPMODEL; Buytaert, 2011) and, based on the increasing frequency with which R appears in peer-reviewed literature, it seems to be earning wide buy-in from the scientific community. Because it is used by so many different disciplines that regularly contribute to the Comprehensive R Archive Network (CRAN), R may uniquely facilitate interdisciplinary collaborations among scientists in numerous fields, (e.g., socioeconomic, political, hydrological, and biological sciences) thus encouraging cross-fertilization of ideas among the traditionally disparate disciplines.

The SWATmodel package we developed provides a linear-model-like R interface to the SWAT modeling system, transforming weather data through a multi-parameter modeling space into a hydrological output response. A valuable feature of R analysis packages is their ability to work on most OS and system architectures. SWATmodel contains the public domain SWAT FORTRAN code, slightly modified to be GNU (GNU's Not Unix), multi-architecture, FORTRAN compiler compliant. This way CRAN can confirm compliance, compile binaries, and distribute the SWAT model for most OS.

Following is an example of a simple implementation within an R session that obtains the necessary information from the US Geological Survey stream gage (ID: 04216500)

to initialize a SWAT model run, and, using the gage coordinates, obtains the necessary weather variables with which to run the model.

```
install.packages("SWATmodel")
library(SWATmodel)
testSWAT2005()
flowgage_id="04216500"
flowgage=get_usgs_gage(flowgage_id)
hist_wx=get_cfsr_latlon(flowgage$declat,flowgage$declon)
build_swat_basic(dirname=flowgage_id,iyr="1979",nbyr=6,flowgage$area,
    flowgage$elev,flowgage$declat,flowgage$declon,hist_wx=hist_wx)
streamflow=SWAT2005(hist_wx)
plot(streamflow$flowdata,flowgage$flowdata)
```

Calibration of SWAT parameters using predicted output and observations can be performed as outlined in the R EcoHydRology package (Fuka et al. 2011) or in Wu and Liu (2012) and is detailed in Appendix B.

REFERENCES

Arnold J.G., Srinivasan R., Muttiah R.S., Williams J.R. 1998. Large area hydrologic modeling and assessment Part I: Model development. Water Resources Bulletin. 34(1):73 89.

Buytaert, W. 2011. TOPMODEL: Implementation of the hydrological model TOPMODEL in R. R package version 0.7.2-2. Available at: http://CRAN.R-project.org/package=topmodel . Accessed: 04/21/2011.

Fuka D.R., Walter M.T., Archibald J.A,, Steenhuis, T.S., Easton Z.M. 2012. EcoHydRology: A community modeling foundation for Eco-Hydrology. R package version 0.4.5. Available at: http://CRAN.R-project.org/package=EcoHydRology . Accessed 08/01/2012

Wu, Y., Liu, S. 2012. Automating calibration, sensitivity and uncertainty analysis of complex models using the R package Flexible Modeling Environment (FME): SWAT as an example. Environmental Modelling & Software, 31:99-109 http://dx.doi.org/10.1016/j.envsoft.2011.11.013

CHAPTER 5

A SIMPLE PROCESS-BASED SNOWMELT ROUTINE TO MODEL SPATIALLY DISTRIBUTED SNOW DEPTH AND SNOWMELT IN THE SWAT MODEL*

Abstract

We present a method to integrate a process-based (PB) snowmelt model that requires only daily temperature and elevation information into the Soil and Water Assessment Tool (SWAT) model. The model predicts the spatio-temporal snowpack distribution without adding additional complexity, and in fact reduces the number of calibrated parameters. To demonstrate the utility of the PB model we calibrate the PB and temperature-index (TI) SWAT models to optimize agreement with stream discharge on a 46km^2 watershed in northwestern Idaho, USA, for 10 individual years and use the calibrated parameters for the year with the best agreement to run the model for 15 remaining yrs. Stream discharge predictions by the PB and TI model were similar, though the PB model simulated snowmelt more accurately than the TI model for the remaining 15-yr period. Spatial snow distributions predicted by the PB model better matched observations from LandSat imagery and a SNOTEL station. Results for this watershed show that including PB snowmelt in watershed models is feasible, and calibration of TI-based watershed models against discharge can incorrectly predict snow cover.

---

* Fuka, D.R., Easton, Z.M., Brooks, E.S., Boll, J., Steenhuis, T.S., Walter, M.T. 2012 A Simple Process-Based Snowmelt Routine to Model Spatially Distributed Snow Depth and Snowmelt in the SWAT Model. Journal of the American Water Resources Association, 1-11. DOI: 10.1111/j.1752-1688.2012.00680.x

Introduction

Snow accumulation and subsequent melt are important hydrologic processes in many arid and semi-arid regions of the world. In areas with high elevations and/or high latitudes, such as much of the western US, up to 80% of the annual streamflow originates from snowpack and snowmelt (Pagano and Garen, 2005; Yarnell et al, 2010). Climate change is expected to result in changes in the hydrology of many regions that have historically depended on snowfall as their primary water source. Thus, researchers rely on watershed models for evaluating possible future changes in hydrology. Unfortunately most of these operational models predict at a scale far too large to capture important hydrological processes (e.g, the SNOw Data Assimilation System-SNODAS of the National Operational Hydrologic Remote Sensing Center uses a 1-km grid resolution), or utilize temperature Index (TI) based methods that require extensive calibration (e.g., Soil and Water Assessment Tool-SWAT model) that cannot be applied outside the range of conditions for which they were calibrated. Incorporating more physically based approaches into watershed models will improve our confidence that results are representative of actual environmental processes and not artifacts of calibration procedures. This is especially important as watershed models are becoming more commonly used for resource planning (Mirchi et al., 2009).

The SWAT model (e.g., Arnold et al., 1998; and Fohrer, 2005) is currently one of the most widely used hydrological models for water resource assessment (e.g., Santhi et al., 2001; van Griensven and Bauwens, 2003; Borah and Bera, 2003; Ramanarayanan

et al., 2005; Gassman et al. 2007; Easton et al., 2010). Although it is often referred to as a "physically based" model (e.g., Srinivasan et al. 2010; White et al. 2011) and, indeed, many of the biogeochemical subroutines in SWAT are 'process-based' (PB), it uses an empirical temperature index (TI) model to predict snowmelt. Using a TI snowmelt model is usually justified by the perceived complexity of obtaining additional meteorological and topographic inputs required in process based energy budget equations (Walter et al. 2005; Zhang et al. 2008). Zhang et al. (2008) demonstrated the benefits of using the National Weather Service (NWS) river forecast center's (RFC) process-based snowmelt model (SNOW17) in un-gauged basins due to the reduced calibration effort, but also found that SNOW17 required extensive modification to SWAT and required significantly more complex forcing variables, i.e., the land surface energy fluxes. It has been shown that SWAT's TI snowmelt model (Fontaine et al. 2002) can be calibrated to generate as accurate stream discharge as the process-based SNOW17 model, with less initialization effort (Zhang et al. 2008; Zeinivand and De Smedt 2009). Debele et al. (2010) present a similar comparison of PB and TI snowmelt models integrated into SWAT2000 and concluded that TI models that consider elevation result in no significant improvement in discharge predictions at the basin outlet over PB models. However, the TI based SWAT (SWAT-TI) had limited capacity for spatially distributing snow accumulation and melt and TI based methods are inherently invalidated when land use or regional climatic changes are introduced since recalibration would be required. The unaddressed issue in these previous studies (Zhang et al., 2008; Debele et al., 2010) is whether TI- or PB-based snow models correctly reproduce the intra-watershed patterns of snow accumulation

and melt. Because snow has profound effects on soil freezing, biogeochemistry, soil moisture patterns, and other processes relevant to water quality, it may be as important to correctly simulate these internal processes as it is to correctly predict discharge at the watershed outlet. Thus, there is a need for models that are easily initialized while remaining inherently process-based. It is useful to recognize that PB models need not be prohibitively data intensive (e.g., Walter et al. 2005) and that simple models may perform as well or better than more complex models for predicting fluxes at the outlet (e.g., Baveye and Boast 1999; Steenhuis et al. 1999; Easton et al. 2011). However, it is critical to correctly predict the internal hydrologic patterns and flows in order to meaningfully model nonpoint source pollution (Dahlke et al. 2009). This is especially true if the model is used to target management strategies for protecting water quality, i.e., the critical parts of the landscape where water flows, and potentially polluting activities coincide (e.g., Moore and Thompson 1996; Frankenberger et al. 1999; Walter et al. 2001, Easton et al. 2008). Thus, correctly predicting flows at a watershed outlet does not indicate that the intra-watershed processes, or the distributions of water are correctly captured by the model (Easton et al. 2011). An added benefit of PB models is that there is, in theory, the ability to physically measure or derive the needed parameters independently, which reduces model calibration. This, of course, has value in areas where there are not extensive data records against which to calibrate the model (e.g., ungaged basins).

Walter et al. (2005) demonstrated that a PB snowmelt model works well without calibration. Thus, incorporating a PB snowmelt model in SWAT (SWAT-PB) would

reduce the number of calibrated parameters compared to the TI method (SWAT-TI). This project explored the benefits of integrating a simple, PB, spatially distributed, snowmelt and snow depth routine within the SWAT2005, SWAT2009, and future versions of the model, requiring no additional data, and only one simple additional initialization step to the current initialization procedures. In order to ensure that the PB snow model addition did not unduly impact the functionality of SWAT, we compare the agreement between modeled and measured stream discharge at the watershed outlet. We also show that while both models are able to perform similarly well at the basin outlet, only the PB model is capable of correctly representing the intra-basin spatial distribution of snow, as indicated with comparison against LandSat imagery and an adjacent SNOTEL station. Our study site was the Paradise Creek watershed, near Moscow, ID; all data used in the models were from publicly available data sources.

SWAT model Description

SWAT is a watershed model that is initialized and run with readily available watershed forcing data, such that general initialization does not require overly complex data gathering. SWAT was originally intended to model long-term runoff and nutrient losses from rural watersheds, particularly those dominated by agriculture (Arnold et al., 1998). Spatial data required to initialize SWAT include soils, land use, and elevation data. In SWAT, hydrologic response units (HRUs) are the smallest predictive unit and are defined by unique combinations of soils classes, land use, and slope classes within a subbasin. For the version of the model used in this study,

SWAT2005, the underlying spatial distribution of the HRUs within a subbasin is effectively ignored, although the latest release (SWAT2009) has made efforts to address this issue (Arnold et al. 2010). Forcing data required for a simulation are precipitation and temperature, though additional forcing data such as solar radiation and wind speed can be included to enhance additional PB solutions within SWAT. Watershed initialization interfaces include ArcSWAT, which requires ESRI ArcGIS Geographical information system (GIS), and MWSWAT, which uses the MapWindow GIS, both of which delineated and initialized the study watershed equally well.

Methods

Walter et al. (2005) demonstrated that many of the meteorological and energy-flux inputs required for a daily PB snowmelt energy balance can be estimated with modest data requirements, e.g., the day of the year, latitude, and daily maximum and minimum temperatures, indicating that a PB approach is not prohibitively data intensive relative to a TI model. We modify the Walter et al. (2005) approach to include the spatial distribution of snowpack in the watershed. The following daily energy balance for a snowpack is used:

$$\frac{\Delta SWE}{\Delta t} = \frac{S+L_a-L_t+H+E+G+P}{\lambda} \qquad \text{for } T_s=0 \qquad (5.1a)$$

$$\frac{\Delta T_S}{\Delta t} = \frac{S+L_a-L_t+H+E+G+P}{C(SWE)} \qquad \text{for } T_s<0 \qquad (5.1b)$$

where $\Delta SWE/\Delta t$ is the change in the snowpack water equivalent (m d^{-1}), S is the net incident solar radiation (kJ m^{-2} d^{-1}), with spatial characterization of hillslopes accounted for by adjusting S for slope and aspect using (eq. 5.2):

$$S = S' (1 + (SIN(\theta) * m) \quad (5.2)$$

where θ is the angle off of true east, m is the slope of the hill in percent, and S' is the potential net incident solar radiation tangent to the earth's normal spheroid. L_a is the atmospheric long wave radiation (kJ m^{-2} d^{-1}), L_t is the terrestrial long wave radiation (kJ m^{-2} d^{-1}), H is the sensible heat exchange (kJ m^{-2} d^{-1}), E is the energy flux associated with the latent heats of vaporization and condensation at the surface (kJ m^{-2} d^{-1}), G is ground heat conduction to the bottom of the snowpack (kJ m^{-2} d^{-1}), P is heat added by rainfall (kJ m^{-2} d^{-1}), SWE is the current day's snowpack water equivalent, C is snowpack specific heat (assumed here to be constant, 0.0021 kJ m23 $^{o}C^{-1}$), $\Delta T_s/\Delta t$ is the change in snowpack temperature (^{o}C d^{-1}), and λ is the latent heat of fusion (3.35 x 10^5 kJ m^{-3}). However, none of these energy fluxes are input directly but, rather, are estimated using just minimum and maximum temperature, latitude, elevation, and time of year (Walter et al. 2005; appendix A).

--Data Sources

Weather data were obtained from the nearest COOP meteorological station (COOP ID: 106152), located within the lower portion of the watershed, with records spanning the period of interest from January 1990 through December 2008. There were 91 days

of missing temperature and precipitation data from 1990-2008. Missing data were estimated using the SWAT weather generator.

The model was initialized with the most accessible datasets for the watershed; when multiple datasets were considered equally accessible, we used the most current. The data sets used were: STATSGO soils dataset (USDA-SCS 1993), a GIS based coverage distributed with the ArcSWAT modeling system. Temperature and precipitation were, obtained from the closest COOP station, "Moscow U Of I" (COOP ID: 106152). The National Elevation Dataset (NED) at 30m cell resolution (Gesch 2007; Gesch et al. 2002) was used for topography and the 2001 Multi-Resolution Land Characteristics (MRLC) Consortium (MRLC 2011) web interface for land use, also at 30m cell resolution (Homer et al. 2004) (available at: Multi-Resolution Land Characteristics Consortium (MRLC) Available at: http://www.mrlc.gov/. Accessed 2/6/2011.).

--Study Site

Since the purpose of this study is to demonstrate intra-subbasin spatial distribution of snow, a watershed where the authors have familiarity with and access to was required. For this reason, the test watershed selected was located above USGS Paradise Creek stream gage (ID 13346800), (USGS, 2011. USGS Real-Time Water Data for USGS 13346800 Available at: http://waterdata.usgs.gov/usa/nwis/uv?13346800. Accessed 2/6/2011) adjacent to the University of Idaho, Moscow, ID (Latah County, Moscow

West quadrangle, Hydrologic Unit 17060108). Recorded discharge (1978-present) ranged from 0.001 m^3s^{-1} to 27 m^3s^{-1} and elevations range from 775m to 1327m.

The Paradise Creek watershed has an area of 4573 ha, with approximately 50% of the watershed classified as Agricultural Land/Row Crops (AGRR), 17% Forest Evergreen (FRSE), 25% Urban Low/Medium/High density and 7% classified as Range-Brush (RNGB). Within the basin 49% of the soils are classified as THATUNA silt loam, 29% SOUTHWICK silt loam, 15% VASSAR silt loam, and 7% TANEY silt loam. There are three slope classes with 34% of the watershed in the range of 0-7% slope, 29% of the watershed in the range of 7-16% slope, and 37% of the watershed greater than 16% slope. Again, since we were interested in assessing the ability of the model to capture the spatial distributions of snow within a watershed, and since we wanted to limit the potential effect of over parameterizing possible by including more subbasins than necessary, we departed from traditional SWAT initialization procedures, and initialized a watershed as a single subbasin. This allowed true rendering of the HRU distribution (e.g., we did not reduce the number of HRUs using the thinning function in the interface), which resulted in 409 HRUs.

--Model Modifications

We created the new PB snowmelt subroutine (owsnowmelt.f) that solves the daily energy balance for a snowpack. We modified the version of the Walter et al. (2005) PB snowmelt routine to include the influences of land use (vegetation), slope, and aspect on incident solar radiation, *S*, and changes in elevation within the subbasin. All

parameters are derived from data currently required to initialize SWAT. We use the daily leaf area index (LAI) calculated in SWAT for canopied land classifications at the hydrologic response unit (HRU) level to adjust solar radiation linearly, where a LAI above 1 results in $S = 0$. Aspect, calculated during the digital elevation model (DEM) processing (using the D8 algorithm of Tarboton, 1997), and slope, are already determined for each HRU and were used to adjust the solar declination value in the calculation of S (i.e., Walter et al. 2005), with true East and West facing slopes considered equivalent to a horizontal plane on the earth's surface.

The effects of forest canopies on the sensible heat exchange (eq. 5.1, H), latent heats of vaporization and condensation at the surface (E), and atmospheric long wave radiation (L_a), were included in SWAT-PB by adjusting the mean wind velocity below forest canopies to 50% of the model supplied wind velocity (Ohta et al., 1999; Oliver, 1971), which reduced eq. 5.1, H and E values accordingly (Walter et al. 2005). In areas of the watershed dominated by evergreen land cover, we assume that long wave radiation from the canopy is much greater than from the atmosphere and the atmospheric long wave radiation L_a was calculated with the Stefan-Botzman equation using the average canopy temperature and an emissivity equal to the LAI for LAI<1 and equal to one for LAI≥1.

Critical for the solution of eq. 5.1 are accurate estimates of temperature and precipitation throughout the watershed, both of which can vary spatially due to subbasin topology. Lapse rates, for both temperature and precipitation, were added

using published values of 10^{o}C/km elevation and 770mm/km elevation, respectively (Bigler et al., 2007; Ahl et al., 2008). Different values may be appropriate in different locations, but these values are either known or can be easily determined, and are often regionally representative. To minimize SWAT code modifications, the temperature and precipitation lapse rates were only included in the new snowmelt routine.

Because the new snowmelt model only required a single new subroutine, owsnowmelt.f, (to replace the current SWAT snowmelt routine, snom.f), only one line of code was modified in the existing surface.f routine, i.e., the line calls the new snowmelt routine instead of the old one. Several variables (surface albedo, snow depth, and snow temperature) had to be tracked through the model run, so two lines in the modparm.f module and four lines to the allocate.f subroutine had to be modified. We also modified the code to permit frozen soil seepage by commenting out the logical test for frozen soil in percmicro.f (from Easton et al. 2008). Finally, the soils were reclassified to include topographic aspects and relative elevation in the watershed into four increments varying from 100m to 400m, with more extreme sloping areas having larger increments; the latter is similar to the method introduced by Easton et al. (2008) for including variable source areas in SWAT using a soil topographic index (STI), although here we integrate elevation ranges as opposed to ranges of STI.

--Calibration

The watershed was calibrated for both SWAT-TI and SWAT-PB versions using the Differential Evolution Optimization library (DEoptim) (Ardia and Mullen, 2009)

within the statistical computing environment R (Ihaka and Gentleman, 1996; RDC Team, 2009). Each of the SWAT2005 parameters (defined in Table 5.1) was defined as either those calibrated by replacement within an initial range published in the literature (Table 5.1, Method column as ”replace”) or those calibrated by adjusting the base initialization default variables by a certain percentage (Table 5.1, Method column as ”percent”). We performed 15 calibrations for 15 individual years within the 1994-2008 period for both SWAT-TI and SWAT-PB. This was done to demonstrate the ability of each model in basins with limited historical data. Ideally we would calibrate each process independently, but this is not the way it is usually done because often we only have discharge data at the watershed outlet and without specific snow data it is infeasible to calibrate the snow model independently of the rest of the hydrological model. It should be noted that calibration of the parameters SFTMP, SMTMP, SMFMX, SMFMN, TIMP was only required for SWAT-TI since SWAT-PB requires no calibration for snow modeling. Soil parameters (Depth, BD, AWC, KSAT), are examples of those in which defaults are perturbed with the DEoptim algorithm to find an optimal calibration. The curve number (CN) and variables controlling ground water (GW_DELAY, ALPHA_BF, QWQMN), and surface and lateral flow parameters (SURLAG, LAT_TTIME), which often change depending on subbasin characteristics, are examples of those in which we set a range from published values and let the DEoptim algorithm hunt for the best result. The local-to-best differential evolution strategy (Price et al. 2005) was used for both the range calibrated and perturbed parameters, with daily predicted vs observed flow Nash Sutcliffe efficiencies (NSE) (Nash and Sutcliffe, 1970) used as the objective function.

Table 5.1. Calibrated parameters used for Differential Evolution Optimization. SFTMP, SMTMP, SMFMX, SMFMN, TIMP being calibrated only for the TI version of SWAT.

Variable	Definition	Method	Range/Percent
SFTMP	Snowfall temperature [C]	replace	-5 – 5 Deg. C
SMTMP	Snow melt base temperature [C]	replace	-5 – 5 Deg. C
SMFMX	Melt factor for snow on June 21 [mm H_2O/C-day]	replace	-5 – 5 Deg. C
SMFMN	Melt factor for snow on December 21 [mm H_2O/C-	replace	-5 – 5 Deg. C
TIMP	Snow pack temperature lag factor	replace	-5 – 5 Deg. C
GW_DELAY	Groundwater delay [days]	replace	1 - 180 Days
ALPHA_BF	Baseflow alpha factor [days]	replace	1 - 180 Days
SURLAG	Surface runoff lag time [days]	replace	1 - 180 Days
GWQMN	Threshold depth of water in the shallow aquifer [mm]	replace	1 - 200 mm
LAT_TTIME	Lateral flow travel time [days]	replace	1 - 180 Days
ESCO	Soil evaporation compensation factor	replace	.2 - .99
CN2	Initial SCS CN II value	replace	65 - 85
Depth	Soil layer depths [mm]	percent	50 – 150 %
BD	Bulk Density Moist [g/cc]	percent	50 – 150 %
AWC	Average available water [mm/mm]	percent	50 – 150 %
KSAT	Saturated conductivity [mm/hr]	percent	50 – 150 %

--Corroboration Methods

Since there are very few spatially distributed snow depth sensors in the study site, corroboration was accomplished with a combination of methods including evaluating the models ability to predict daily discharge at the watershed outlet, comparing the modeled SWE to the nearest active SNOTEL station, visual corroboration against LandSat imagery, and analytical comparison of spatial depth with LandSat pixel brightness.

Corroboration of the calibrated models at the outlet was performed by running the best single year calibration for each model from 1990-2008 period, and comparing measured against daily simulated basin outflow for the period of 1994-2008. 1990 – 1993 was used as the warm-up period for which the model is allowed to reach numerical equilibrium.

Data from the SNOTEL station located above the highest point of the Paradise Cr. Drainage (1327m) was compared to the closest HRU elevation increment within the modeled basin. SNOTEL Site 989 (USGS, 2010. Moscow Mountain (989) - Site Information and Reports. Available at: http://www.wcc.nrcs.usda.gov/nwcc/site?sitenum=989&state=id. Accessed 9/20/2010.), Moscow Mountain in Latah county ID, at 1433m has reported since the beginning of the snow year 2000. Though the station only has records for the last 8 years of the study period and is approximately 100m above the highest point in the

watershed (300m above the average elevation of the highest elevation increment in the watershed, or 1116m), it is used as a reference point to demonstrate snow accumulation at higher altitude in the evergreen forested HRU's for the basin. The influence of aspect on the modeled SWE is corroborated by comparing a time series of SWE modeled with SWAT-PB and SWAT-TI for HRU's sharing the same characteristics except topographic aspect.

LandSat imagery with limited cloud cover and a pass over the watershed during the simulation period was obtained. Visual determination of snow absence and presence by slope aspect was made by comparison of the LandSat image against the model predicted snow distribution (at the HRU level). Visual corroboration of the snow distribution was performed against a single panchromatic LandSat 7 channel (channel 8), which shows relative brightness of 15 m resolution pixels. We used the true-color combination of the Red (channel 3, 0.63 - 0.69μm), Green (channel 2, 0.52 - 0.60μm) and Blue (channel 1, 0.45 - 0.52μm) LandSat 7 channels to identify an image day that exhibited obvious, heterogeneous spatial snow distribution (April 4, 2008); note, directly comparing the true-color images to model simulations was not very valuable because the true-color images are at a coarser resolution, 30m, and are not aligned with datasets that the HRUs are developed from.

We assumed that brighter LandSat 7 pixels correlated with deeper snowdepths in the April 4, 2008 image, (i.e., during the spring melt season, we correlated predicted snowdpeths to the LandSat image brightness). We tested the spatial predictive ability

of snow distribution in SWAT-PB using two approaches. First, at the HRU-scale, the mean of the LandSat 7 panchromatic normalized brightness for all pixels within each HRU polygon were compared against the associated modeled snow depth. We used a linear regression to determine the goodness of fit between the estimated (LandSat 7) and modeled SWAT-PB snow distribution. Secondly, at the pixel-scale, the modeled SWE (a polygonal dataset) was rasterized to the same resolution of the LandSat 7 panchromatic channel image (15 m), and the resulting raster map was processed with a Gaussian filter to smooth out the sharp transitions that occur at HRU's polygon boundaries. The rasterized, modeled snowdepths were then binned into 10 evenly distributed bins to develop a box plot graphical analysis.

Results and Discussion

--Calibration results and sensitivity ranges

The average optimal calibrated parameter values for the sixteen parameters determined for each of the 15 individual calibration years are shown in Table 5.2. Mean NSE for the 15 individual calibration years of daily discharge data were slightly higher (though not statistically different) for the SWAT-PB model [NSE of 0.54 (Standard Deviation (SD)=0.24)] than for the SWAT-TI model [0.51 (SD=0.24)] (Table 5.2). The differences between SWAT-PB- and SWAT-TI model parameters were all within the 1 SD ranges of each other; the soil parameters, depth, bulk density, available water capacity, and saturated hydraulic conductivity were very similar between the two models (Table 5.2).

Table 5.2. Summary mean and standard deviation of the resulting NSE performance and individual parameter ranges for 15 sets of single year calibrations. PB indicates the SWAT-PB model results, TI indicates the SWAT-TI model results, PB-TI indicates the difference between SWAT-PB minus SWAT-TI values. Not Applicable (NA's) are placed where a parameter is not used for the SWAT-PB model.

	Mean			Standard Deviation			Coefficient of Variation		Paired t-test
Snow Model	**PB**	**TI**	**PB-TI**	**PB**	**TI**	**PB-TI**	**PB**	**TI**	**p-value**
NSE	0.54	0.51	0.03	0.24	0.24	-0.01	0.44	0.47	
Calibration Parameters									
CN2	70.45	73.21	-2.76	5.77	6.45	-0.68	0.08	0.09	0.380
SFTMP	NA	-1.27	NA	NA	2.62	NA	NA	-2.06	NA
SMTMP	NA	0.02	NA	NA	3.62	NA	NA	181.00	NA
SMFMX	NA	-1.62	NA	NA	2.67	NA	NA	-1.65	NA
SMFMN	NA	-0.27	NA	NA	3.41	NA	NA	-12.63	NA
TIMP	NA	0.15	NA	NA	3.13	NA	NA	20.87	NA
ESCO	0.55	0.50	0.05	0.18	0.19	-0.01	0.33	0.38	0.885
Depth	0.95	1.02	-0.07	0.28	0.23	0.05	0.29	0.23	0.582
BD	1.07	1.13	-0.06	0.30	0.29	0.01	0.28	0.26	0.240
AWC	1.15	1.11	0.04	0.26	0.31	-0.05	0.23	0.28	0.406
KSAT	1.11	1.05	0.05	0.29	0.27	0.02	0.26	0.26	0.495
LAT_TIME	46.92	71.57	-24.65	44.86	49.92	-5.07	0.96	0.70	0.869
GWQMN	92.30	81.82	10.48	50.71	37.34	13.37	0.55	0.46	0.980
ALPHA_BF	118.83	72.78	46.05	49.61	51.15	-1.55	0.42	0.70	0.197
GW_DELA	82.13	86.92	-4.79	53.29	41.03	12.25	0.65	0.47	0.253
SURLAG	73.59	96.76	-23.17	44.95	61.80	-16.85	0.61	0.64	0.585

Interestingly, the variability in the calibrated parameters values over the 15 year-by-year calibrations was similar between the two models as shown with a paired t-test grouped by calibration, with the exception of the snow parameters, SFMP, SMTMP, SMFMX, and SMFMN, which needed no calibration in SWAT-PB (see coefficients of variation in Table 5.2). For SWAT-TI, the variability in the calibrated snow parameters was one to four orders of magnitude greater than any of the other parameters (Table 5.2).

--Stream discharge corroboration

After determining the optimal calibrated values (based on stream discharge) for all parameters and both models for each of 15 individual years, each specific calibration parameter set was run and compared to measured daily stream flow for the entire range of years 1994-2008. In general, SWAT-PB performed substantially better than SWAT-TI, mean NSE of 0.45 and 0.32, respectively (Table 5.3). However, the best NSE for SWAT-TI, 0.60, was slightly higher than the best SWAT-PB run, 0.58 (Table 5.3). Though not statistically different, the differences between the models were much greater for the poorer performing simulation; the lowest NSE for the SWAT-TI was -0.11 was substantially lower than the worst SWAT-PB run, NSE=0.18.

--Snow depth corroboration

Figure 5.1 compares the SWAT predicted *SWE* for water years 2001-2008 using parameters from the best calibration-year for SWAT-TI and SWAT-PB (1997 and 2003, respectively) and SNOTEL measure *SWE* (note that the SNOTEL station is

Table 5.3. Corroboration Results, summary of the 15 yearly calibrations corroborated against stream flow from 1994-2008

	PB	TI
Mean NSE	0.42	0.32
Max NSE	0.58	0.60
Min NSE	0.25	-0.11
SD NSE	0.10	0.18

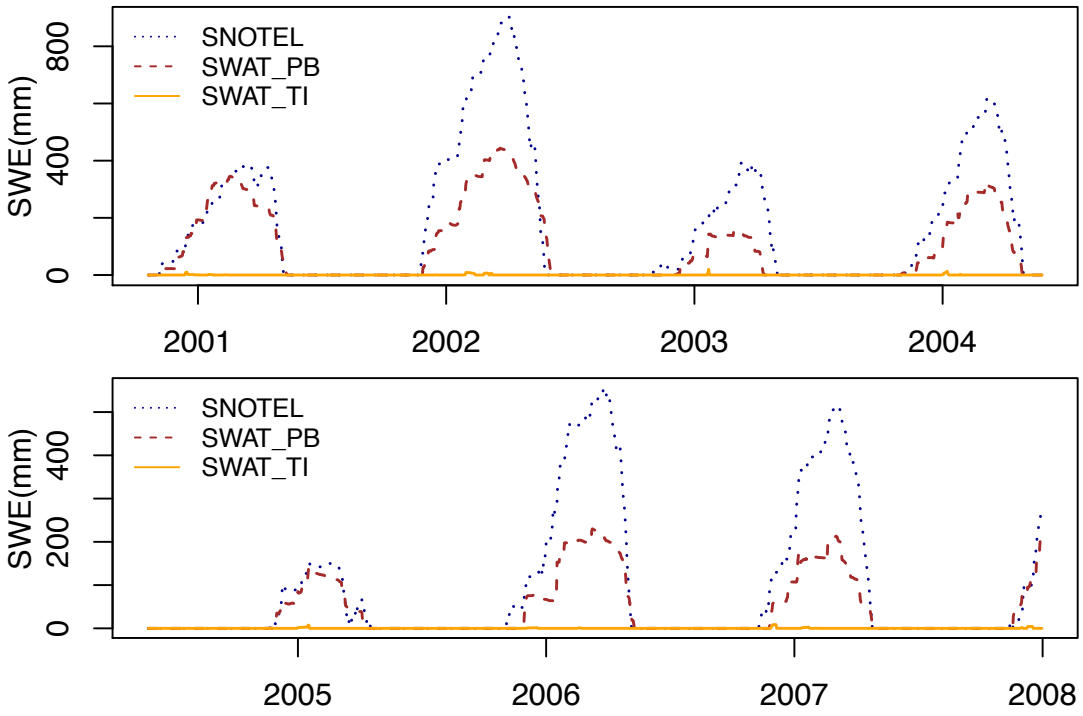

Figure 5.1. SWE for HRU 185, An evergreen forest at the highest elevation in the watershed for water years 2001 - 2008. Blue dotted line is SNOTEL measured, 300m above the average elevation of the highest elevation increment in the watershed, dashed brown line is BP, and orange line is optimal calibration for TI**.**

100m above the watershed). In Fig. 5.1 it is evident that the optimum calibration of the SWAT-TI model resulted in almost no snow accumulation over this period. This highlights the importance of recognizing that a model's capacity to reproduce flow at the outlet, i.e., the data used to optimize the calibration, does not imply that the internal processes or spatial patterns are correctly simulated. Here, the calibration of SWAT-TI produced parameter values for the groundwater and runoff processes that gave better agreement between modeled and measured stream flow than could be achieved via snow accumulation and melt; note, there were too many parameter combinations to determine precisely which parameter values off-set the lack of modeled snow accumulation. As is expected, because calibration is unnecessary, the PB-model accumulates and melts snow, no matter what the outcome of autocalibration. In Fig. 5.1, as expected, the timing of the annual accumulation and melt cycles for the PB-model coincide well with the measured snow accumulation and melt measured at the SNOTEL gauge but the magnitude of snow accumulation is lower because the highest HRU is below the SNOTEL, i.e., we expect more snow accumulation at higher elevations.

--Corroboration of the spatial distribution of snow

In Fig. 5.2, we visually compare the snow visible within the LandSat 7 scene from April 4, 2008 (Fig. 5.2a) with the predicted snow depth for both SWAT-PB (Fig. 5.2b) and SWAT-TI (Fig. 5.2c). Strips of missing data present in Fig. 5.2a are a result of the May 2003 Scan Line Corrector failure in the ETM+ instrument. While this represents only a single day during the 10 year model run it represents some of the only

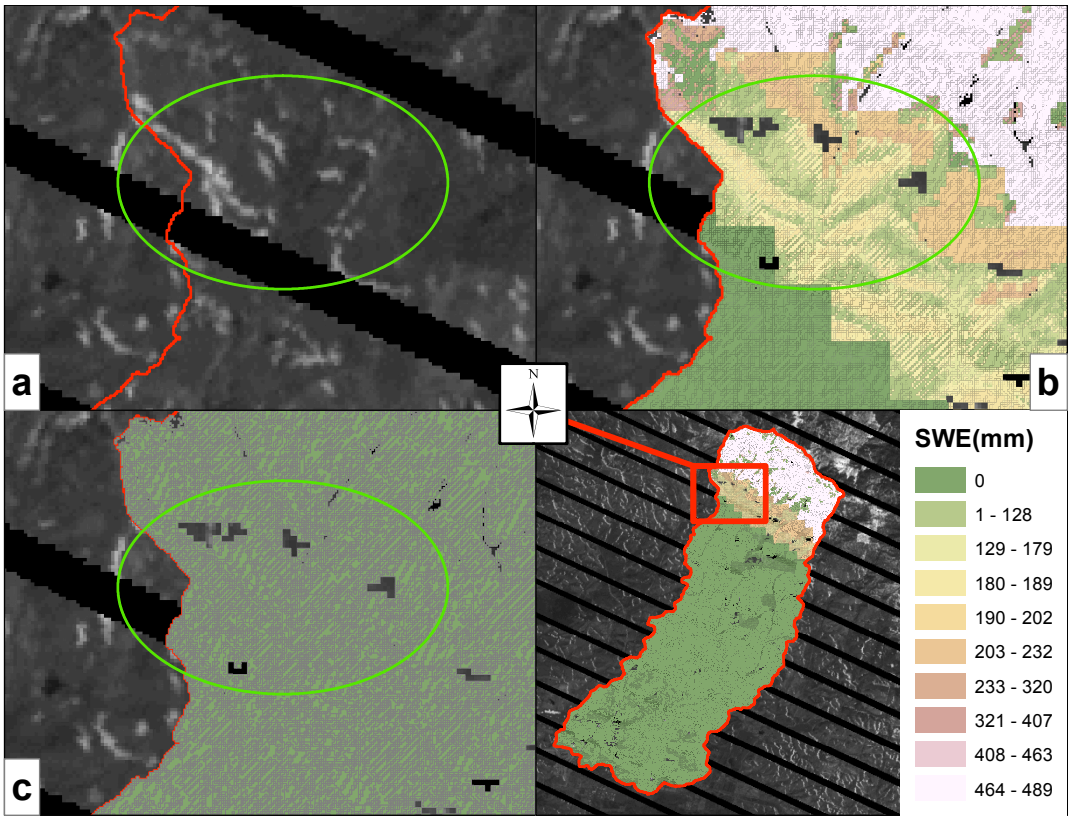

Figure 5.2. Spatial corroboration using LandSat 7 imagery from April 3, 2008 with oval highlighting the same area in each scene. Upper left frame(a) LandSat 7 distinctly shows hillslope snow distribution. Upper right frame(b), SWAT-PB distinctly shows linear features of hillside snow that align with the LandSat 7 imagery. Lower left (c) SWAT-TI shows relatively uniform snow distribution.

available, high resolution spatial data, and it is difficult to find scenes that are capable of distinguishing the influence of aspect on snow distribution. Figure 5.2c shows the snow depth for the entire subbasin in the SWAT-TI model, and it is clear that there is little snow, and that it does not vary spatially, using the optimal calibration run for SWAT-TI (calibration year 1997). In Fig. 5.2c there are no significant differences in SWAT-TI predicted snow depth among land uses, slopes, and aspects. SWAT-PB results (Fig. 5.2b) show a more realistic distribution of snowpack with differences in snow depth on north- verses south-facing slopes and, as expected, more snow at higher elevations and in the evergreen forest (Fig. 5.2b). The elevation effects are abrupt due to the way elevation was incremented into four elevation groups, but increasing the number of elevation groups in the initialization would result in a more continuous and gradual increase in snow depth with elevation.

Figure 5.3 confirms SWAT-PB's ability to predict the impact of aspect on snow distribution throughout a snow year. In this comparison, we grouped all HRUs that had the same elevation, slope, land use, and soils, with the differentiating factor being the direction the slope is facing. This allows a comparison of the influence of aspect in the model. Cleary shown in Fig. 5.3, is that SWAT-PB maintains snowpack longer and at a greater depth on north facing slopes than on south facing slopes, which is intuitive as north facing slopes receive less incident solar radiation, but is none-the-less ignored in SWAT-TI.

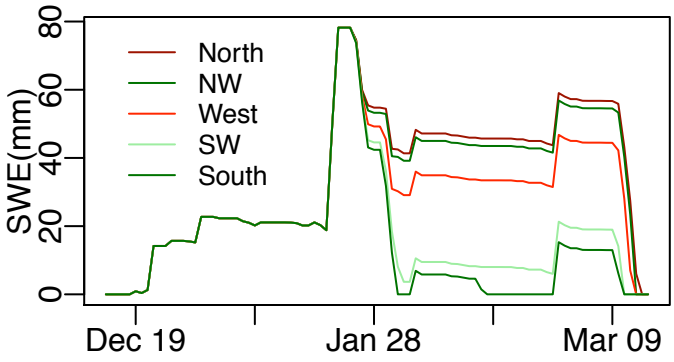

Figure 5.3. SWAT-PB model results for HRU Snow Water Equivalent (SWE), distinguished by hillslope aspect.

After visual corroboration of the spatial distribution of snow in the watershed, we perform an analytical comparison of the SWAT-PB model results against the LandSat 7 imagery. Using the same LandSat 7 scene as was used for the visual comparison, a linear regression of modeled *SWE* against the LandSat 7 panchromatic brightness performed from the perspective of the polygonal HRU data set (Fig. 5.4a) demonstrates the relationship between mean pixel brightness and SWAT-PB modeled *SWE,* and although there is significant variation at values of low *SWE*/pixel brightness, SWAT-PB is able to capture the general trend. Figure 5.4b further demonstrates this relationship from a raster cell perspective, and again is reassuringly able to capture the expected trend. Figure 5.4 also highlights the complexities of determining snow depth using remote sensing as variable illumination, detector saturation and other impediments make determining not only the presence or absence, but also the depth and *SWE* of snow complex (Rosenthal and Dozier, 1996).

Summary and Conclusions

This study demonstrates that a simple PB snowmelt model can be incorporated into an existing operational hydrologic model with little change to the original code base and without adding substantial input data requirements. On a 46km^2 watershed in northern Idaho, USA, we demonstrate this by incorporating an energy budget, PB snow model into SWAT2005 using only readily available data, e.g., maximum and minimum daily temperature, geographic latitude, and published values for physical parameters, e.g., latent heat of fusion, snow heat capacity, etc. SWAT2005 actually has the capacity to directly use many parameters that were estimated in this study; for example solar

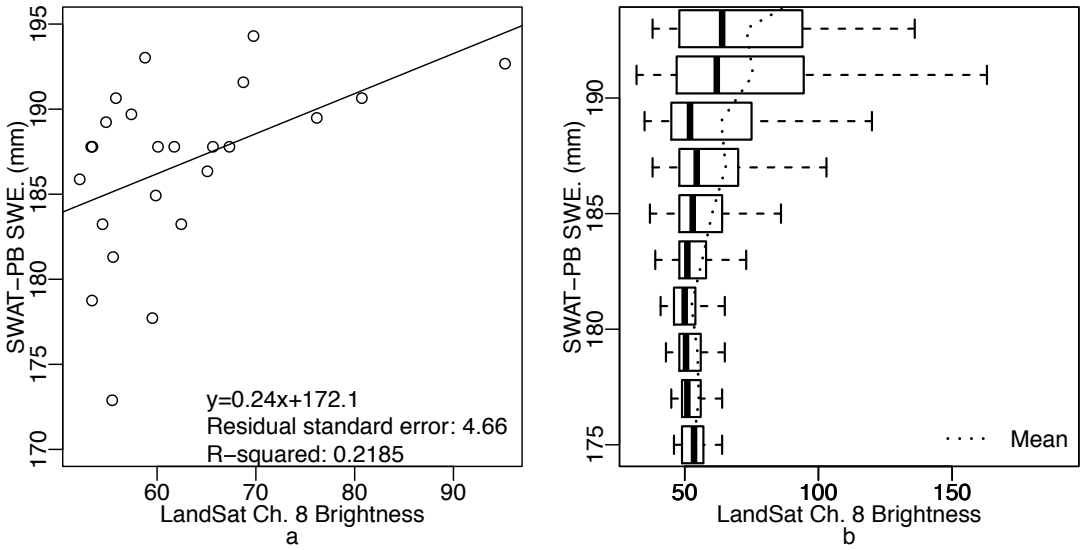

Figure 5.4. Left(a) HRU-based comparison of SWAT-PB *SWE* (mm) vs LandSat 7 Channel 8 panchromatic brightness. Mean for each polygon extracted from raster LandSat 7 scene. Right (b) Raster cell based comparison of SWAT-PB *SWE*(mm) vs LandSat 7 Channel 8 panchromatic brightness with boxplots showing the progression of grouped means and pixel spread.

radiation, wind, and humidity and we expect that SWAT-PB would perform better than demonstrated here if these were used directly when and/or where these data exist. Because this study was performed using many independent one-year calibrations, we were able to show the high degree of variability in the calibrated TI parameters from year to year, emphasizing the need for process-based models when limited or no data is available (i.e. ungaged basins). For this watershed, it was interesting to discover that the optimal calibrated parameter set for SWAT-TI actually resulted in simulating no snow some years, despite direct observations and measurements that show snow accumulation and melt every year. This indicates that calibrating a TI model against only watershed outlet discharge may necessarily misrepresent other hydrologic processes, as the error in one of the most important hydrologic processes can only be compensated for with induced errors in other processes. Overall, this study affirms that calibrating hydrological models to watershed outlet discharge may not ensure internal processes and patterns of water distribution are correctly simulated, that spatial snowmelt does not require extensive model modification, and that the complexity of data requirements need not be a hurdle for those processes dependent on the surface energy budget. Fine resolution distributed snow data in more watersheds are required to further test the model proposed here. One final note, while we have focused on snowmelt/accumulation as it relates to the energy budget, we envision methods such as these to be applicable to a number of different, relevant hydrologic processes.

Supporting Information

Additional Supporting Information may be found in the online version of this article: owsnowmelt.f, a FORTRAN subroutine written in format, data structure, and paradigm of SWAT2005 and SWAT2009 source code with minor modification to surface.f, modparm.f, and allocate.f .

Acknowledgements

LandSat 7 Enhanced Thematic Mapper Plus (ETM+) courtesy of the U.S. Geological Survey.

This material is based upon work supported by Synthesis and Analysis of 13 CSREES CEAP Projects and the Cooperative State Research, Education and Extension Service, US Department of Agriculture, under agreement No. 2007-51130-03992.

REFERENCES

Ahl, R.S., Woods, S.W., Zuuring, H.R. 2008. Hydrologic calibration and validation of SWAT in a snow-dominated rocky mountain watershed, Montana, USA. Journal of the American Water Resources Association, 44(6):1411-1430.

Ardia, D., Mullen, K. 2009. DEoptim: Differential evolution optimization in R. R package version 2.0-3. Available at: http://CRAN.R-project.org/package=DEoptim. Accessed 09/03, 2010.

Arnold, J.G., Gassman, P.W., White, M.J. 2010. New developments in the SWAT ecohydrology model. In: Proceedings of the Watershed Technology Conference, February 21-24, American Society of Agricultural and Biological Engineers, Earth University, Costa Rica.

Arnold, J.G., Srinivasan, R., Muttiah, R.S., Williams, J.R. 1998. Large area hydrologic modeling and assessment - Part I: Model development. Water Resources Bulletin, 34(1):73-89.

Arnold, J.G., Fohrer, N. 2005. Preface: SWAT2000: Current capabilities and research opportunities in applied watershed modelling. Hydrological Processes, 19(3):563-572.

Baveye, P., Boast, C.W. 1999. Physical scales and spatial predictability of transport processes in the environment. Geophysical Monograph, 108:261-280.

Bigler, C., Gavin, D.G., Gunning, C., Veblen, T.T. 2007. Drought induces lagged tree mortality in a subalpine forest in the Rocky Mountains. Oikos, 116(12):1983-1994.

Borah, D.K., Bera, M. 2003. Watershed-scale hydrologic and nonpoint-source pollution models: Review of mathematical bases. Transactions of the ASABE, 46(6):1553-1566

Dahlke, H.E., Easton, Z.M., Fuka, D.R., Lyon, S., Steenhuis, T.S. 2009. Developing and testing a semi-distributed model to predict saturated area dynamics in an agriculturally dominated watershed. Ecohydrology, 2(3): 337-349.

Debele B., Srinivasan R., Gosain A.K. 2010. Comparison of Process-based and temperature-index snowmelt modeling in SWAT. Water Resources Management, 24(6):1065-1088.

Easton, Z.M., Fuka, D.R., Walter, M.T., Cowan, D.M., Schneiderman, E.M., Steenhuis, T.S. 2008. Re-conceptualizing the soil and water assessment tool (SWAT) model to predict runoff from variable source areas. Journal of Hydrology, 348(3-4):279-291.

Easton, Z.M., Fuka, D.R., White, E.D, Collick, A.S., Ashagre, B.B, McCartney, M., Awulachew, S.B., Ahmed, A.A., Steenhuis, T.S. 2010. A multi basin SWAT model analysis of runoff and sedimentation in the Blue Nile, Ethiopia. Hydrology and Earth System Science, 14:1827-1841. doi:10.5194/hess-14-1827-2010, 2010.

Easton, Z.M., Walter, M.T., Fuka, D.R., White, E.D., Steenhuis, T.S. 2011. A simple concept for calibrating runoff thresholds in quasi-distributed variable source area watershed models. Hydrological Processes, 25(20):3131-3143, doi:10.1002/hyp.8032, 2011.

Fontaine, T., Cruickshank, T., Arnold, J., Hotchkiss, R. 2002. Development of a snowfall–snowmelt routine for mountainous terrain for the Soil Water Assessment Tool (SWAT). Journal of Hydrology, 262(1-4):209-223.

Frankenberger, J.R., Brooks, E.S., Walter, M.T., Walter, M.F. 1999. A GIS-based variable source area hydrology model. Hydrological Processes, 13(6):804-822.

Gassman, R.W., Reyes, M.R., Green, C.H., Arnold, J.G. 2007. The Soil and Water Assessment Tool: Historical development, applications, and future research directions. Transactions of the ASABE, 50(4):1211-1250.

Gesch, D.B. 2007. "Chapter 4 – The National Elevation Dataset", in Maune, D., ed., Digital Elevation Model Technologies and Applications: The DEM Users Manual, 2nd Edition: American Society for Photogrammetry and Remote Sensing, Bethesda, Maryland.

Gesch D., Oimoen M., Greenlee S., Nelson C., Steuck M., Tyler D., 2002. The National Elevation Dataset. Photogrammetric Engineering and Remote Sensing, 68(1):5-11.

van Griensven A., Bauwens, W. 2003. Concepts for river water quality processes for an integrated river basin modeling. Water Science and Technology, 48(3):1-8.

Homer, C., Huang, C., Yang, L., Wylie, B., Coan, M. 2004. Development of a 2001 national landcover database for the United States. Photogrammetric Engineering and Remote Sensing, 70:829-840.

Ihaka, R., Gentleman R. 1996. R: A language for data analysis and graphics. Journal of Computational and Graphical Statistics, 5(3):299-314.

Mirchi, A., Watkins, Jr., D., Madani, K. 2009. “Chapter 6 – Modeling for watershed planning, management, and decision making”, in: Vaughn J.C., (Eds.), Watersheds:

management, restoration, and environmental impact. Nova Science Publishers, New York. pp. 221-224

Moore, R.D., Thompson, J.C. 1996. Are water table variations in a shallow forest soil consistent with the TOPMODEL concept? Water Resources Research, 32(3):663-669.

Nash, J.E., Sutcliffe, J.V. 1970. River flow forecasting through conceptual models part I — A discussion of principles. Journal of Hydrology, 10(3):282-290.

Ohta, T., Suzuki, K., Kodama,Y., Kubota, J., Kominami, Y., Nakai, Y. 1999. Characteristics of the heat balance above the canopies of evergreen and deciduous forests during the snowy season. Hydrological Processes, 13(14-15):2383-2294.

Oliver, H. 1971. Wind profiles in and above a forest canopy. Quarterly Journal of the Royal Meteorological Society, 97(414):548-553.

Pagano T., Garen, D. 2005. A recent increase in western US streamflow variability and persistence. Journal of Hydrometeorology, 6(2):173-179.

Price K.V., Storn, R.M., Lampinen, J.A. 2005. Differential evolution: A practical approach to global optimization (Natural Computing Series). Springer-Verlag. Berlin, Heidelberg.

Ramanarayanan, T., Narasimhan, B., Srinivasan, R. 2005. Characterization of fate and transport of isoxaflutole, a soil-applied corn herbicide, in surface water using a watershed model. Journal of Agricultural and Food Chemistry, 53(22):8848-8858.

RDC Team. 2009. R: A Language and Environment for Statistical Computing. Available: http://www.R-project.org. Accessed 1 January 2010.

Rosenthal, W., Dozier, J. 1996. Automated mapping of montane snow cover at subpixel resolution from the Landsat Thematic Mapper. Water Resources Research, 32(1):115-130.

Santhi, C., Arnold, J.G., Williams, J.R., Dugas, W.A., Srinivasan, R., Hauck L.M. 2001. Validation of the SWAT model on a large river basin with point and nonpoint sources. Journal of the American Water Resources Association, 37:1169-1188.

Srinivasan, R., Zhang, X., Arnold, J. 2010. SWAT ungauged: Hydrological budget and crop yield predictions in the upper Mississippi River basin. Transactions of the ASABE, 53(5):1533-1546.

Steenhuis, T.S., Parlange, J.Y., Sanford, W.E., Heilig, A., Stagnitti, F., Walter, M.F. 1999. Can we distinguish Richards' and Boussinesq's equations for hillslopes?: The Coweeta experiment revisited. Water Resources Research, 35(2):589-593.

Tarboton, D.G. 1997. A new method for the determination of flow directions and upslope areas in grid digital elevation models, Water Resources Research, 33(2):309–319.

U.S. Department of Agriculture, Soil Conservation Service (USDA-SCS). 1993. STATSGO data users guide. Miscellaneous Publication Number 1492.

Walter, M.T., Parlange, J.Y., Walter, M.F., Xin, X., Scott, C.A. 2001. Modeling pollutant release from a surface source during rainfall runoff. Journal of Environmental Quality, 30(1):151–159

Walter, M.T., Brooks, E.S., McCool, D.K., King, L.G., Molnau, M., Boll, J. 2005. Process-based snowmelt modeling: does it require more input data than temperature-index modeling? Journal of Hydrology, 300(1-4):65-75.

White, E.D., Easton, Z.M., Fuka, D.R., Collick, A.S., Adgo, E., McCartney, M., Awulachew, S.B., Selassie, Y.G., Steenhuis, T.S. 2011. Development and application of a physically based landscape water balance in the SWAT model. Hydrological Processes, 25:915-925. doi:10.1002/hyp.7876, 2011.

Yarnell, S.M., Viers, J.H., Mount, J.F. 2010. Ecology and management of the spring snowmelt recession. Bioscience, 60(2):114-127.

Zeinivand, H., De Smedt, F. 2009. Hydrological modeling of snow accumulation and melting on river basin scale. Water Resources Management, 23(11):2271-2287.

Zhang, X., Srinivasan, R., Debele, B., Hao, F. 2008. Runoff simulation of the headwaters of the Yellow River using the SWAT model with three snowmelt algorithms. Journal of the American Water Resources Association, 44(1):48-61.

APPENDIX A

DATA SOURCES FOR CHAPTER 2

Daily stream flow and CFSR weather data for each basin can be obtained using the following CRAN distributed EcoHydRology package using the following script where the stream flow is stored in the "flowgage" list and the CFSR data is stored in the "weather" dataframe:

```
# Install and load the libraries
install.packages("EcoHydRology")
library(EcoHydRology)

# Flow and CFSR for Cross River, NY, USA
flowgage_id="01374890"
flowgage=get_usgs_gage(flowgage_id)
weather=get_cfsr_latlon(flowgage$declat,flowgage$declon)

# Flow and CFSR for Tesuque Cr. NM, USA
flowgage_id="08302500"
flowgage=get_usgs_gage(flowgage_id)
weather=get_cfsr_latlon(flowgage$declat,flowgage$declon)

# Flow and CFSR for Andreas Cr., CA, USA
flowgage_id="10259000"
flowgage=get_usgs_gage(flowgage_id)
weather=get_cfsr_latlon(flowgage$declat,flowgage$declon)

# Flow and CFSR for Town Brook NY, USA
flowgage_id= "01421618"
flowgage=get_usgs_gage(flowgage_id)
weather=get_cfsr_latlon(flowgage$declat,flowgage$declon)

# CFSR for Gumara, Ethiopia
weather=get_cfsr_latlon(11.747042,37.797672)
```

Stream flow for the Gumara is available from the ministry of water resources at:

`http://www.mowr.gov.et/`

Weather station data for the region surrounding the Gumara is available at the National Meteorology Agency of Ethiopia:

`http://www.ethiomet.gov.et/`

APPENDIX C

A FORTRAN SUBROUTINE WRITTEN IN FORMAT, DATA STRUCTURE, AND PARADIGM OF SWAT2005 AND SWAT2009 SOURCE CODE FOR CHAPTER 5

```
      subroutine owsnowmelt

!!    ~ ~ ~ PURPOSE ~ ~ ~
!!    this subroutine predicts daily snom melt when the average air
!!    temperature exceeds 0 degrees Celcius

!!    ~ ~ ~ INCOMING VARIABLES ~ ~ ~
!!    name         |units         |definition
!!    ~ ~ ~ ~ ~ ~ ~ ~ ~ ~ ~ ~ ~ ~ ~ ~ ~ ~ ~ ~ ~ ~ ~ ~ ~ ~ ~ ~ ~ ~ ~ ~ ~ ~ ~
!!    iida         |julian date   |day being simulated (current julian date)
!!    ihru         |none          |HRU number
!!    precipday    |mm H2O        |precipitation on the current day in the HRU
!!    sno_hru(:)   |mm H2O        |amount of water in snow in HRU on current day
!!    snoeb(:,:)   |mm H2O        |snow water content in elevation band on
!!                                |current day
!!    snotmp(:)    |deg C         |temperature of snow pack in HRU
!!    snotmpeb(:,:)|deg C         |temperature of snow pack in elevation band
!!    timp         |none          |Snow pack temperature lag factor (0-1)
!!                                |1 = no lag (snow pack temp=current day air
!!                                |temp) as the lag factor goes to zero, the
!!                                |snow pack's temperature will be less
!!                                |influenced by the current day's air
!!                                |temperature
!!    tmpav(:)     |deg C         |average air temperature on current day for
!!                                |HRU
!!    tmx(:)       |deg C         |maximum air temperature on current day for
!!    tmn(:)       |deg C         |minimum temperature for the day in HRU
!!    snam(:)      |NA            |soil series name, with included D8 and Elevation
!!    ~ ~ ~ ~ ~ ~ ~ ~ ~ ~ ~ ~ ~ ~ ~ ~ ~ ~ ~ ~ ~ ~ ~ ~ ~ ~ ~ ~ ~ ~ ~ ~ ~ ~ ~
!!    ~ ~ ~ OUTGOING VARIABLES ~ ~ ~
!!    name         |units         |definition
!!    ~ ~ ~ ~ ~ ~ ~ ~ ~ ~ ~ ~ ~ ~ ~ ~ ~ ~ ~ ~ ~ ~ ~ ~ ~ ~ ~ ~ ~ ~ ~ ~ ~ ~ ~
!!    hhprecip(:)  |mm H2O        |precipitation falling during hour in day
!!    precipday    |mm H2O        |amount of water in effective precipitation
!!                                |in HRU
!!    precipdt(:)  |mm H2O        |precipitation for the time step during day
!!    sno_hru(:)   |mm H2O        |amount of water in snow in HRU on current day
!!    snoeb(:,:)   |mm H2O        |snow water content in elevation band on
!!                                |current day
!!    snofall      |mm H2O        |amount of precipitation falling as freezing
!!                                |rain/snow on day in HRU
!!    snomlt       |mm H2O        |amount of water in snow melt for the day in
!!                                |HRU
!!    snotmp(:)    |deg C         |temperature of snow pack in HRU
!!    snotmpeb(:,:)|deg C         |temperature of snow pack in elevation band
!!    ~ ~ ~ ~ ~ ~ ~ ~ ~ ~ ~ ~ ~ ~ ~ ~ ~ ~ ~ ~ ~ ~ ~ ~ ~ ~ ~ ~ ~ ~ ~ ~ ~ ~ ~

!!    ~ ~ ~ LOCAL DEFINITIONS ~ ~ ~
!!    name        |units         |definition
!!    ~ ~ ~ ~ ~ ~ ~ ~ ~ ~ ~ ~ ~ ~ ~ ~ ~ ~ ~ ~ ~ ~ ~ ~ ~ ~ ~ ~ ~ ~ ~ ~ ~ ~ ~
!!    albmax      |Decimal %    |Max Snow Albedo = .95
!!    j           |none          |HRU number
!!    owtmpav     |deg C         |average air temperature on current day for
!!                               |HRU adjusted for lapse rate/altitude
!!    soldec      |radians       |solar declination
!!    snc         !degree/45     |D8 direction off of east
!!    snel        |1/100m        |Elevation change from meteorological station
!!    1k30dsw_pot |kJ/m^2        |30 day sum of potential solar radiation
!!    sw_pot      |kJ/m^2        |extraterestrial potential solar radiation
!!    latrad      |radians       |latitude of location in radians
```

```
!!    iida_mo_ago |Julien Date   |Julien Date - 30
!!    at_tr       |Decimal %     |atmospheric transmisivity
!!    b_emp       |None          |emperical fitting coef
!!    alb         |Decimal %     |albedo
!!    alb_decl(:) |Decimal %     |albedo at the start when SWE drops below .3m
!!    albprev(:)  |Decimal %     |albedo on previous day in hru
!!    newsno      |Decimal %     | equiv water depth of new snow fall
!!    newsno_den  |Decimal %     |density of the new snow
!!    sw_netnet   |kJ/m^2        |incident short wave
!!    lw_t        |kJ/m^2        |lw_terestrial
!!    cc          |Decimal %     |cloud cover
!!    ea          |kJ/m^2        |atmospheric emissivity
!!    lw_at       |kJ/m^2        |atmospheric long wave
!!    sh          |kJ/m^2        |sensible heat exchange
!!    heat_resist |day/m         |resistance to heat transfer possibly using
!!                               |http://rredc.nrel.gov/wind/pubs/atlas/maps.html#2-7
!!                               | as a reference for wind speed
!!    ~ ~ ~ ~ ~ ~ ~ ~ ~ ~ ~ ~ ~ ~ ~ ~ ~ ~ ~ ~ ~ ~ ~ ~ ~ ~ ~ ~ ~ ~ ~ ~ ~ ~ ~ ~ ~
!!   Note: For simplification against published methodology, Radiation budjet is
!!   calculated in kJ/m^2 and multiplied by 1000 to give units of mm.
!!    ~ ~ ~ ~ ~ ~ END SPECIFICATIONS ~ ~ ~ ~ ~ ~
      use parm
      implicit none
      real, parameter :: PI=3.141592653589793D0
      integer :: j,ii,iida_mo_ago,snc,snel
      real :: swconst,slope_dec
      real :: snowdens,newsno_den,latrad, soldec,heat_resist
      real :: lw_at,alb,sw_net,lw_t,cc,ea,sh,prevsnotmp,rho_s
      real :: k_month_sw_pot,b_emp,at_tr,sw_pot,rho_a,ef,gh,ph,swecdt
      real :: del_swe,owtmpav,albmax,ulocal
!! initialize local variables
      j = 0
      j = ihru
      albmax=.95
!!
!! Read the D8 aspect, HRU aspect (snc) and elevation (snel) from the soil name.
!! Currently, we imbed these characteristics in the soil layer as we wish not to
!! alter the base SWAT modeling system.
!!
      read(snam(j),'(2I1)') snc,snel
!! Temperature Lapse Rate
!! Watch out here, currently the lapse rate is set to .5*snel, due to a our
!! setting of 1=100m. In the future we neeed to make this set from input lapse rates.
!!
      owtmpav=tmpav(j) - real(snel)*1.60
!! Calculate snow fall
!! Currently the ppt lapse rate is set to 1+.3*snel, due to a 60% rate change from
bottom
!! to top of example watershed. In the future we can set from the input lapse rate.
!! (Bigler, 2007; Ahl, 2008)
      if (owtmpav <= 0.0) then
        sno_hru(j) = sno_hru(j)+precipday*(1.0 +real(snel)*0.2)
        snofall = precipday *(1.0 +real(snel)*0.2)
        precipday = 0.
        hhprecip(:) = 0.
        precipdt(:) = 0.
      else
        snofall = 0.0
      endif
!!
!!  Solutions from here to Balance see Walter et al. 2005
!!  unless otherwise noted.
!!
!!  Solar Radiation
!!
      swconst=117.5e3
      if (sub_lat(hru_sub(j)) < 1.e-4) sub_lat(hru_sub(j)) =            &
     &    wlat(hru_sub(j))
      latrad = sub_lat(hru_sub(j)) / 57.296

      iida_mo_ago=iida-30
```

```
      if (iida_mo_ago<0) iida_mo_ago=365+iida_mo_ago
      soldec=.4102*sin(2*3.1416/365*(iida_mo_ago-80))
      k_month_sw_pot=swconst/3.1416*(acos(-tan(soldec)*tan(latrad))*    &
     &    sin(latrad)*sin(soldec) + cos(latrad)*cos(soldec)*            &
     &    sin(acos(-tan(soldec)*tan(latrad))))/1000.0

      slope_dec=-SIN((real(snc)-1.0)*PI*2.0/8.0)*hru_slp(j)
      soldec=.4102*sin(2*3.1416/365*(iida-80)) + slope_dec

      if((soldec+latrad)>(PI/2.).or.(-tan(soldec)*tan(latrad)).ge.1.0)  &
     &  then
        sw_pot=0.0
      else
        sw_pot=swconst/3.1416*(acos(-tan(soldec)*tan(latrad))*          &
     &    sin(latrad)*sin(soldec) + cos(latrad)*cos(soldec)*            &
     &    sin(acos(-tan(soldec)*tan(latrad))))
      endif


      if (iida .ge. 83 .and. iida .le. 263) then
         b_emp=.282*latrad**(-.431)
      else
         b_emp=.170*latrad**(-.979)
      endif
      at_tr=.75*(1-exp(-b_emp/k_month_sw_pot*(tmx(j)-tmn(j))**2))

      if(alb_decl(j)<=.01)alb_decl(j)=.8
      if(albprev(j)<=.01)albprev(j)=.8
      snowdens=.4
      if (snofall .gt. 0.0) then
        newsno_den=50.+3.4*(owtmpav+15.)
        alb=.95-(.95-albprev(j))*exp(-(4.0*snofall/
     &    newsno_den/.12))
        alb_decl(j)=alb
        sno_decl(j)=sno_hru(j)
      elseif (sno_hru(j)< 300.) then
        if(sno_decl(j) .gt. 0.0 .and. sno_hru(j).gt.0.0) then
          alb=alb_decl(j)-(alb_decl(j)-.25)*(sno_decl(j)-sno_hru(j))/     &
     &       sno_decl(j)
        else
          alb=.25
        endif
      else
        alb=.35-(.35-.95)*exp(-1.0*(.177+ (alog((.95-.35) /                  &
     &   (albprev(j)-.35)))**2.16)**.46)
        alb_decl(j)=alb
        sno_decl(j)=sno_hru(j)
      endif
      albprev(j)=alb
      sw_net=(1.0-alb)*at_tr*sw_pot*(1.0-min(laiday(j),1.0))

!!
!!  Long Wave Radiation, Terrestrial
!!
!! ERROR IN PAPER stefan boltsman constan
      lw_t=.97*4.9e-6*(owtmpav+273.)**4
!!
!!  Long Wave Radiation, Atmospheric
!!
      cc=(1.0-at_tr/.75)
      if(idplt(1,1,ihru).eq.8) then
        ea=.9
      else
        ea=MAX(0.0000092*(owtmpav+273)**2,(0.0000092*(owtmpav+273)**2
     &     +0.005*owtmpav)*(1-0.84*cc)+0.84*cc)
      endif
      lw_at=ea*4.9e-6*(owtmpav+273.)**4
!!
!!  Heat from convective vapor exchange.
!!  for tree canopies, we set u=20%*u per {{52 Ohta, T. 1999;}} {{54 Oliver, HR
1971;}}.
```

```
!!
      if(idplt(1,1,ihru).eq.8) then
        ulocal=.50*u10(j)
      else
        ulocal=u10(j)
      endif
      heat_resist=.0044578/ulocal
      sh=-1.29*(snotmp(j)-owtmpav)/heat_resist
!!
!! Estimate snow pack temperature
!!
      prevsnotmp= snotmp(j)
      snotmp(j) = snotmp(j) * (1. - timp) + owtmpav * timp
      if (snotmp(j) >0.0)snotmp=0.0
      rho_s= exp((16.78*snotmp(j)-116.8)/(snotmp(j)+273.3))/((273.15+   &
     &      snotmp(j))*.4615)
      rho_a= exp((16.78*owtmpav-116.8)/(owtmpav+273.3))/((273.15+       &
     &      owtmpav)*.4615)
      ef=2500*(rho_s-rho_a) / heat_resist
!!
!!  Ground heat conduction.
!!

      gh=173.0
!!
!!  Precipitation heat.
!!
      ph=0.0
      if (owtmpav >= 0.0 ) then
        ph=4.2E3*owtmpav*precipday/1000.0
      endif
!!
!!  Stored Snowpack Energy
!!
      swecdt= 2.1*(snotmp(j)-prevsnotmp)*sno_hru(j)/1000.0
!!
!! Balance
!!
      del_swe=1.0/3.35E5*(sw_net+lw_at-lw_t+sh-ef+gh+ph-swecdt)

      if (del_swe < 0.) del_swe = 0.
      if (del_swe*1000.0 > sno_hru(j)) del_swe = sno_hru(j)/1000.0
      sno_hru(j)= sno_hru(j) - del_swe*1000.0
      snomlt=del_swe*1000.0
!  This addition to precipday is post precipday being set to 0.0 due to
!  snowfall. This allows melt to runoff even if snow was accumilated
!
      precipday = precipday + del_swe*1000.0
      if (precipday < 0.) precipday = 0.
      if (nstep > 0) then
        do ii = 1, 24
         hhprecip(ii) = hhprecip(ii) +  del_swe/ 24
        end do
        do ii = 1, nstep
         precipdt(ii+1) = precipdt(ii+1) +  del_swe / nstep
        end do
      end if
      snoeb(:,j)=sno_hru(j)
      snotmpeb(:,j)=snotmp(j)
 5000 format(a10,i4,22(a8,1x,e10.3))
 5001 format(a10,i4,i4,22(a8,1x,e10.3))

      return
      end
```

APPENDIX C

A FORTRAN SUBROUTINE WRITTEN IN FORMAT, DATA STRUCTURE, AND PARADIGM OF SWAT2005 AND SWAT2009 SOURCE CODE FOR CHAPTER 5

```
      subroutine owsnowmelt

!!    ~ ~ ~ PURPOSE ~ ~ ~
!!    this subroutine predicts daily snom melt when the average air
!!    temperature exceeds 0 degrees Celcius

!!    ~ ~ ~ INCOMING VARIABLES ~ ~ ~
!!    name         |units         |definition
!!    ~ ~ ~ ~ ~ ~ ~ ~ ~ ~ ~ ~ ~ ~ ~ ~ ~ ~ ~ ~ ~ ~ ~ ~ ~ ~ ~ ~ ~ ~ ~ ~ ~ ~ ~
!!    iida         |julian date   |day being simulated (current julian date)
!!    ihru         |none          |HRU number
!!    precipday    |mm H2O        |precipitation on the current day in the HRU
!!    sno_hru(:)   |mm H2O        |amount of water in snow in HRU on current day
!!    snoeb(:,:)   |mm H2O        |snow water content in elevation band on
!!                                |current day
!!    snotmp(:)    |deg C         |temperature of snow pack in HRU
!!    snotmpeb(:,:)|deg C         |temperature of snow pack in elevation band
!!    timp         |none          |Snow pack temperature lag factor (0-1)
!!                                |1 = no lag (snow pack temp=current day air
!!                                |temp) as the lag factor goes to zero, the
!!                                |snow pack's temperature will be less
!!                                |influenced by the current day's air
!!                                |temperature
!!    tmpav(:)     |deg C         |average air temperature on current day for
!!                                |HRU
!!    tmx(:)       |deg C         |maximum air temperature on current day for
!!    tmn(:)       |deg C         |minimum temperature for the day in HRU
!!    snam(:)      |NA            |soil series name, with included D8 and Elevation
!!    ~ ~ ~ ~ ~ ~ ~ ~ ~ ~ ~ ~ ~ ~ ~ ~ ~ ~ ~ ~ ~ ~ ~ ~ ~ ~ ~ ~ ~ ~ ~ ~ ~ ~ ~
!!    ~ ~ ~ OUTGOING VARIABLES ~ ~ ~
!!    name         |units         |definition
!!    ~ ~ ~ ~ ~ ~ ~ ~ ~ ~ ~ ~ ~ ~ ~ ~ ~ ~ ~ ~ ~ ~ ~ ~ ~ ~ ~ ~ ~ ~ ~ ~ ~ ~ ~
!!    hhprecip(:)  |mm H2O        |precipitation falling during hour in day
!!    precipday    |mm H2O        |amount of water in effective precipitation
!!                                |in HRU
!!    precipdt(:)  |mm H2O        |precipitation for the time step during day
!!    sno_hru(:)   |mm H2O        |amount of water in snow in HRU on current day
!!    snoeb(:,:)   |mm H2O        |snow water content in elevation band on
!!                                |current day
!!    snofall      |mm H2O        |amount of precipitation falling as freezing
!!                                |rain/snow on day in HRU
!!    snomlt       |mm H2O        |amount of water in snow melt for the day in
!!                                |HRU
!!    snotmp(:)    |deg C         |temperature of snow pack in HRU
!!    snotmpeb(:,:)|deg C         |temperature of snow pack in elevation band
!!    ~ ~ ~ ~ ~ ~ ~ ~ ~ ~ ~ ~ ~ ~ ~ ~ ~ ~ ~ ~ ~ ~ ~ ~ ~ ~ ~ ~ ~ ~ ~ ~ ~ ~ ~

!!    ~ ~ ~ LOCAL DEFINITIONS ~ ~ ~
!!    name        |units         |definition
!!    ~ ~ ~ ~ ~ ~ ~ ~ ~ ~ ~ ~ ~ ~ ~ ~ ~ ~ ~ ~ ~ ~ ~ ~ ~ ~ ~ ~ ~ ~ ~ ~ ~ ~ ~
!!    albmax      |Decimal %    |Max Snow Albedo = .95
!!    j           |none          |HRU number
!!    owtmpav     |deg C         |average air temperature on current day for
!!                               |HRU adjusted for lapse rate/altitude
!!    soldec      |radians       |solar declination
!!    snc         !degree/45     |D8 direction off of east
!!    snel        |1/100m        |Elevation change from meteorological station
!!    1k30dsw_pot |kJ/m^2        |30 day sum of potential solar radiation
!!    sw_pot      |kJ/m^2        |extraterestrial potential solar radiation
!!    latrad      |radians       |latitude of location in radians
```

```
!!    iida_mo_ago |Julien Date   |Julien Date - 30
!!    at_tr       |Decimal %     |atmospheric transmisivity
!!    b_emp       |None          |emperical fitting coef
!!    alb         |Decimal %     |albedo
!!    alb_decl(:) |Decimal %     |albedo at the start when SWE drops below .3m
!!    albprev(:)  |Decimal %     |albedo on previous day in hru
!!    newsno      |Decimal %     | equiv water depth of new snow fall
!!    newsno_den  |Decimal %     |density of the new snow
!!    sw_netnet   |kJ/m^2        |incident short wave
!!    lw_t        |kJ/m^2        |lw_terestrial
!!    cc          |Decimal %     |cloud cover
!!    ea          |kJ/m^2        |atmospheric emissivity
!!    lw_at       |kJ/m^2        |atmospheric long wave
!!    sh          |kJ/m^2        |sensible heat exchange
!!    heat_resist |day/m         |resistance to heat transfer possibly using
!!                               |http://rredc.nrel.gov/wind/pubs/atlas/maps.html#2-7
!!                               | as a reference for wind speed
!!    ~ ~ ~ ~ ~ ~ ~ ~ ~ ~ ~ ~ ~ ~ ~ ~ ~ ~ ~ ~ ~ ~ ~ ~ ~ ~ ~ ~ ~ ~ ~ ~ ~ ~ ~ ~ ~
!!   Note: For simplification against published methodology, Radiation budjet is
!!   calculated in kJ/m^2 and multiplied by 1000 to give units of mm.
!!    ~ ~ ~ ~ ~ ~ END SPECIFICATIONS ~ ~ ~ ~ ~ ~
      use parm
      implicit none
      real, parameter :: PI=3.141592653589793D0
      integer :: j,ii,iida_mo_ago,snc,snel
      real :: swconst,slope_dec
      real :: snowdens,newsno_den,latrad, soldec,heat_resist
      real :: lw_at,alb,sw_net,lw_t,cc,ea,sh,prevsnotmp,rho_s
      real :: k_month_sw_pot,b_emp,at_tr,sw_pot,rho_a,ef,gh,ph,swecdt
      real :: del_swe,owtmpav,albmax,ulocal
!! initialize local variables
      j = 0
      j = ihru
      albmax=.95
!!
!! Read the D8 aspect, HRU aspect (snc) and elevation (snel) from the soil name.
!! Currently, we imbed these characteristics in the soil layer as we wish not to
!! alter the base SWAT modeling system.
!!
      read(snam(j),'(2I1)') snc,snel
!! Temperature Lapse Rate
!! Watch out here, currently the lapse rate is set to .5*snel, due to a our
!! setting of 1=100m. In the future we neeed to make this set from input lapse rates.
!!
      owtmpav=tmpav(j) - real(snel)*1.60
!! Calculate snow fall
!! Currently the ppt lapse rate is set to 1+.3*snel, due to a 60% rate change from
bottom
!! to top of example watershed. In the future we can set from the input lapse rate.
!! (Bigler, 2007; Ahl, 2008)
      if (owtmpav <= 0.0) then
        sno_hru(j) = sno_hru(j)+precipday*(1.0 +real(snel)*0.2)
        snofall = precipday *(1.0 +real(snel)*0.2)
        precipday = 0.
        hhprecip(:) = 0.
        precipdt(:) = 0.
      else
        snofall = 0.0
      endif
!!
!!  Solutions from here to Balance see Walter et al. 2005
!!  unless otherwise noted.
!!
!!  Solar Radiation
!!
      swconst=117.5e3
      if (sub_lat(hru_sub(j)) < 1.e-4) sub_lat(hru_sub(j)) =            &
     &    wlat(hru_sub(j))
      latrad = sub_lat(hru_sub(j)) / 57.296

      iida_mo_ago=iida-30
```

```
      if (iida_mo_ago<0) iida_mo_ago=365+iida_mo_ago
      soldec=.4102*sin(2*3.1416/365*(iida_mo_ago-80))
      k_month_sw_pot=swconst/3.1416*(acos(-tan(soldec)*tan(latrad))*    &
     &    sin(latrad)*sin(soldec) + cos(latrad)*cos(soldec)*            &
     &    sin(acos(-tan(soldec)*tan(latrad))))/1000.0

      slope_dec=-SIN((real(snc)-1.0)*PI*2.0/8.0)*hru_slp(j)
      soldec=.4102*sin(2*3.1416/365*(iida-80)) + slope_dec

      if((soldec+latrad)>(PI/2.).or.(-tan(soldec)*tan(latrad)).ge.1.0)  &
     &  then
        sw_pot=0.0
      else
        sw_pot=swconst/3.1416*(acos(-tan(soldec)*tan(latrad))*          &
     &    sin(latrad)*sin(soldec) + cos(latrad)*cos(soldec)*            &
     &    sin(acos(-tan(soldec)*tan(latrad))))
      endif


      if (iida .ge. 83 .and. iida .le. 263) then
         b_emp=.282*latrad**(-.431)
      else
         b_emp=.170*latrad**(-.979)
      endif
      at_tr=.75*(1-exp(-b_emp/k_month_sw_pot*(tmx(j)-tmn(j))**2))

      if(alb_decl(j)<=.01)alb_decl(j)=.8
      if(albprev(j)<=.01)albprev(j)=.8
      snowdens=.4
      if (snofall .gt. 0.0) then
        newsno_den=50.+3.4*(owtmpav+15.)
        alb=.95-(.95-albprev(j))*exp(-(4.0*snofall/
     &    newsno_den/.12))
        alb_decl(j)=alb
        sno_decl(j)=sno_hru(j)
      elseif (sno_hru(j)< 300.) then
        if(sno_decl(j) .gt. 0.0 .and. sno_hru(j).gt.0.0) then
          alb=alb_decl(j)-(alb_decl(j)-.25)*(sno_decl(j)-sno_hru(j))/     &
     &       sno_decl(j)
        else
          alb=.25
        endif
      else
        alb=.35-(.35-.95)*exp(-1.0*(.177+ (alog((.95-.35) /                  &
     &   (albprev(j)-.35)))**2.16)**.46)
        alb_decl(j)=alb
        sno_decl(j)=sno_hru(j)
      endif
      albprev(j)=alb
      sw_net=(1.0-alb)*at_tr*sw_pot*(1.0-min(laiday(j),1.0))

!!
!!  Long Wave Radiation, Terrestrial
!!
!! ERROR IN PAPER stefan boltsman constan
      lw_t=.97*4.9e-6*(owtmpav+273.)**4
!!
!!  Long Wave Radiation, Atmospheric
!!
      cc=(1.0-at_tr/.75)
      if(idplt(1,1,ihru).eq.8) then
        ea=.9
      else
        ea=MAX(0.0000092*(owtmpav+273)**2,(0.0000092*(owtmpav+273)**2
     &     +0.005*owtmpav)*(1-0.84*cc)+0.84*cc)
      endif
      lw_at=ea*4.9e-6*(owtmpav+273.)**4
!!
!!  Heat from convective vapor exchange.
!!  for tree canopies, we set u=20%*u per {{52 Ohta, T. 1999;}} {{54 Oliver, HR
1971;}}.
```

```
!!
      if(idplt(1,1,ihru).eq.8) then
        ulocal=.50*u10(j)
      else
        ulocal=u10(j)
      endif
      heat_resist=.0044578/ulocal
      sh=-1.29*(snotmp(j)-owtmpav)/heat_resist
!!
!! Estimate snow pack temperature
!!
      prevsnotmp= snotmp(j)
      snotmp(j) = snotmp(j) * (1. - timp) + owtmpav * timp
      if (snotmp(j) >0.0)snotmp=0.0
      rho_s= exp((16.78*snotmp(j)-116.8)/(snotmp(j)+273.3))/((273.15+   &
     &      snotmp(j))*.4615)
      rho_a= exp((16.78*owtmpav-116.8)/(owtmpav+273.3))/((273.15+       &
     &      owtmpav)*.4615)
      ef=2500*(rho_s-rho_a) / heat_resist
!!
!!  Ground heat conduction.
!!

      gh=173.0
!!
!!  Precipitation heat.
!!
      ph=0.0
      if (owtmpav >= 0.0 ) then
        ph=4.2E3*owtmpav*precipday/1000.0
      endif
!!
!!  Stored Snowpack Energy
!!
      swecdt= 2.1*(snotmp(j)-prevsnotmp)*sno_hru(j)/1000.0
!!
!! Balance
!!
      del_swe=1.0/3.35E5*(sw_net+lw_at-lw_t+sh-ef+gh+ph-swecdt)

      if (del_swe < 0.) del_swe = 0.
      if (del_swe*1000.0 > sno_hru(j)) del_swe = sno_hru(j)/1000.0
      sno_hru(j)= sno_hru(j) - del_swe*1000.0
      snomlt=del_swe*1000.0
!  This addition to precipday is post precipday being set to 0.0 due to
!  snowfall. This allows melt to runoff even if snow was accumilated
!
      precipday = precipday + del_swe*1000.0
      if (precipday < 0.) precipday = 0.
      if (nstep > 0) then
        do ii = 1, 24
         hhprecip(ii) = hhprecip(ii) +  del_swe/ 24
        end do
        do ii = 1, nstep
         precipdt(ii+1) = precipdt(ii+1) +  del_swe / nstep
        end do
      end if
      snoeb(:,j)=sno_hru(j)
      snotmpeb(:,j)=snotmp(j)
 5000 format(a10,i4,22(a8,1x,e10.3))
 5001 format(a10,i4,i4,22(a8,1x,e10.3))

      return
      end
```